https://ntrs.nasa.gov/search.jsp?R=19700002358 2020-03-12T04:48:30+00:00Z

N 70 11662

NASA CONTRACTOR
REPORT

Report No. 61312

CASE FILE
COPY

STATIC AND DYNAMIC CALIBRATIONS OF MSFC's PLUG-NOZZLE SPECIAL TEST SECTION (REDESIGNED 1967)

By S. V. Paranjape, J. J. McGowen III, and H. A. Cikanek, Jr.

Nortronics-Huntsville
Northrop Corporation
6025 Technology Drive, P.O. Box 1484
Huntsville, Alabama 35805

January 1969

Prepared for

NASA-GEORGE C. MARSHALL SPACE FLIGHT CENTER
Marshall Space Flight Center, Alabama 35812

TECHNICAL REPORT STANDARD TITLE PAGE

1. REPORT NO.	2. GOVERNMENT ACCESSION NO.	3. RECIPIENT'S CATALOG NO.
NASA CR-61312		

4. TITLE AND SUBTITLE	5. REPORT DATE
STATIC AND DYNAMIC CALIBRATIONS OF MSFC'S PLUG-NOZZLE SPECIAL TEST SECTION (REDESIGNED 1967)	January 1969
	6. PERFORMING ORGANIZATION CODE
7. AUTHOR(S)	8. PERFORMING ORGANIZATION REPORT #
S. V. Paranjape, J. J. McGowen III*, and H. A. Cikanek, Jr.	TR-794-9-433
9. PERFORMING ORGANIZATION NAME AND ADDRESS	10. WORK UNIT NO.
Nortronics-Huntsville Northrop Corporation 6025 Technology Drive, P. O. Box 1484 Huntsville, Alabama 35805	11. CONTRACT OR GRANT NO. NAS8-20082
12. SPONSORING AGENCY NAME AND ADDRESS	13. TYPE OF REPORT & PERIOD COVERED
NASA-George C. Marshall Space Flight Center Marshall Space Flight Center, Alabama 35812	Contractor Report
	14. SPONSORING AGENCY CODE

15. SUPPLEMENTARY NOTES

*Mr. McGowen was an employee of the George C. Marshall Space Flight Center, at the time this research was done.

16. ABSTRACT

This report presents static calibration and evaluation of the dynamic response characteristics of MSFC's 14-inch wind tunnel plug-nozzle special test section, which was redesigned in 1967. This test was performed to calibrate the facility in support of the wind tunnel aerodynamic cross-beam program and to provide pre-test information necessary for conduction of fluctuating pressure experiments. Mach number distribution across the test section flow annulus was determined, and measured deviations were found to be well within instrumentation error. A range of test section Mach numbers from M = 1.97 to 2.78 were investigated in the study and are shown to vary linearly with hand-crank settings. The hand crank is gear-linked to a movable outer wall and regulates throat area with respect to a fixed plug, and, hence, Mach number.

The test revealed unwanted correlated photometer output fluctuations, which were probably caused by mechanical vibrations of the outer wall, periodic pressure fluctuations in the window cavity and the acoustic environment outside the tunnel. These vibrations caused large noise and meaningless correlated fluctuations in the signal. We now know from later tests that such adverse signal components could have been reduced by modifying the electronics and the recording process. Since the shortcomings in the crossed-beam electronics have now been overcome a new test to determine the feasibility of making successful crossed-beam measurements in the special test section may be warranted.

17. KEY WORDS	18. DISTRIBUTION STATEMENT
	PUBLIC RELEASE E. D. Geissler E. D. GEISSLER, Director Aero-Astrodynamics Lab, MSFC

19. SECURITY CLASSIF. (of this report)	20. SECURITY CLASSIF. (of this page)	21. NO. OF PAGES	22. PRICE
U	U	78	

MSFC - Form 3292 (May 1969)

ACKNOWLEDGEMENTS

The authors gratefully acknowledge the kind consideration and assistance provided by the following people: Dr. Krause's leadership and helpful suggestions in the cross-beam program are greatly appreciated. K. D. Johnston's leadership, as project engineer, is acknowledged. Appreciation is expressed to J. L. Sims, D. O. Barnett and J. J. Love for the special test section design calculations and drawings. K. D. Johnston, H. W. Belew and R. J. Love are commended for design and drawings of models. We thank E. H. Simon for use of the facility and for his assistance in designing the soft mounts for instrumentation. J. P. Heaman, H. T. Bush, J. B. Wilbanks, and G. W. Thompson's efforts in design and installation of instrumentation are appreciated. We express our thanks to S. R. Mallard, J. Magnan, and the Northrop Blow-Down Unit for expert operation of the facility. We also appreciate the photographic skills of F. D. Kroelinger. Finally, we would like to express our gratitude to J. B. Thomison and the other Co-op students who participated in the data reduction.

SUMMARY

This report presents static calibration and evaluation of the dynamic response characteristics of MSFC's 14-inch wind tunnel plug-nozzle special test section (redesigned 1967). This test was performed to calibrate the facility in support of the wind tunnel aerodynamic crossed-beam* program and to provide pretest information necessary for conduction of fluctuating pressure tests.

Mach number was found to vary only slightly across the test section flow annulus and the measured deviation was well within the range of instrumentation error for each position of the nozzle outerwall investigated. The range of nominal Mach numbers examined were M=1.97 to 2.78. These were shown to vary linearly with the Mach number control device (movement of outerwall with respect to a fixed centerplug). Convection speeds were measured to be 80 percent of the free stream speed by pairs of transducers separated in the axial direction, corroborating results of other, similar investigations (9).

Determination of steady state run duration of the special test section with varying Mach numbers and model configurations was also an objective of the study. It was found that a minimum of 18 seconds of run time was available. This was estimated to be of adequate length for all presently conceived crossed-beam tests to be conducted in this facility.

Dynamic calibration consisted of fluctuating pressure and acceleration measurements at various locations along the length of the centerplug and in the test section. These instruments were grouped into three regions; the subsonic or upstream portion of the plug, along and inside the plug-extension and the test cavity enclosed by the windows and the outerwall. RMS pressure fluctuations measured in the subsonic region of the plug appear to be high

*Crossed-beam is an optical technique for remote sensing of turbulent flow fields by cross correlation of electro-magnetic radiation.

(148 to 154 db) and eddy scales are apparently large based on qualitative estimates by comparison of 1/4 inch and 1/8 inch diameter transducer results. Thus, it is estimated that the present turbulence damping screens are inadequate, or could at least be substantially improved through modification.

The magnitude of the RMS pressure fluctuations in the supersonic regime (plug-extension) are considerable lower than those in the subsonic regime. Acceleration of the plug was measured by accelerometers to be only 2 g's; thus, structural vibrations of the plug do not appear to be severe.

Very high accelerations were measured on the outerwall (up to 28 g's at M=2), indicating severe vibration. Also strong periodic pressure fluctuations from 1200 to 1600 Hz were found in the window cavity.

It is believed that the severe mechanical vibration of the outerwall, the periodic pressure fluctuations of window cavity, and the acoustic environment of the test cell constitute obstacles (though not insurmountable) to successful measurement of flow phenomenon by the crossed-beam system. However, additional precautions, such as isolation mounting of crossed-beam instrumentation and filtering of photometer outputs are recommended to insure that the measurements are flow related.**

**During a subsequent test (TWT 395, ref. 12, appendix B) an attempt to obtain meaningful crossed-beam measurements in this facility was made. The data were found to be dominated by a periodic frequency of about 1400 Hz; which was probably due to flow-induced, mechanical vibration of the facility. It was later found during a systematic investigation of the crossed-beam instrumentation that several problems existed in the electronics at the time of test TWT 395 (which are reported in the same reference 12, appendix C). Since the problems in the crossed-beam electronics have now apparently been solved, it appears that a new test may determine the feasibility of making successful crossed-beam measurements in the special test section.

TABLE OF CONTENTS

LIST OF ILLUSTRATIONS

LIST OF ILLUSTRATIONS (Continued)

LIST OF ILLUSTRATIONS (Concluded)

NOMENCLATURE

Major Mathematical and Physical Symbols

C	Coefficient of Pressure, Centigrade, or Counter Dial Setting, (depends on Subscripts, superscripts, etc.)
CPS	Cycles per Second
d	Axial Distance between Transducers
db	Decibels
F	Fahrenheit
f	Frequency
g	Gravitational Constant (32.174 ft/sec^2)
hp	Horse Power
Hz	Hertz (cycles per second)
K	1000 times
KC	Kilocycles
M	Mach Number
mv	Millivolts
mm	Millimeter
P	Pressure
PSI	Pounds per Square inch
q	Dynamic Pressure - $(\frac{1}{2}\rho V^2)$
RMS	Root Mean Square
U	Speed
V	Velocity
v	Volts
Δ	Change in
ρ	Density
τ	Time Lag
ϕ	Anguler position of rake in test section flow annulus
	(Note: rake was always canted 30 degrees to the radius as it was rotated through ϕ - see Figure 2-5)

NOMENCLATURE (Concluded)

Mathematical Subscripts

C	Convection
E	Outerwall Exit
L	Local
N	Nominal
p	Plug, probe
R	Rake, also refers to Mach number measurements calculated by static-to-total pressure by use of rake probes only
S	Static
T	Total
X	Referenced to Horizontal Coordinates
Y	Referenced to Vertical Coordinates
0	Stagnation Value, Measured Upstream of Throat
∞	Referenced to Free-Stream Condition

Superscripts

i	Position of Rake Probe by Number (i.e., 1, 2, 3, ..., i)
°	Degrees

Non-Mathematical Symbols

A, G, C, E	Accelerometers
A1	Charge Amplifier
A2	Kistler Amplifier
A3	Tektronix Preamplifiers
B	Temperature Compensators
CEC	Consolidated Electrodynamics Corp. (Brand Name)
SEL	Systems Engineering Laboratory (Brand Name)
STS	Special Test Section
TR	Transducer
TWT	Transonic Wind Tunnel

Section I
INTRODUCTION

The plug-nozzle special test section (MSFC Drawing Number GM543272) of Marshall Space Flight Center's 14- by 14-Inch Wind Tunnel has been modified to be acceptable for proposed cross-beam and fluctuating pressure studies of separated flows over steps, protuberances, and base flows of clustered-nozzle models. The original Special Test Section (designed in 1959) was found to contain discontinuities in the distribution of the wall pressure and was unacceptable for these experiments. New center plug and outerwall contours were generated by applying a method of characteristic solution. The following equipment modifications were also made:

- A new center plug was installed with a diameter reduced from eight to five inches (nominal) to reduce flow blockage due to step and protuberance models, and the overall contour was re-machined.
- Facilities for injecting tracer material in the portion of the flow which experiences the phenomena of separation were added.
- Screens were installed in the entrance region of the nozzle to reduce turbulence level in the test section.
- Top and bottom glass windows were enlarged to facilitate additional vertical beam traverse.

Shakedown tests of this special test section had two major objectives. The first objective was to establish operational procedures for employment of the special test section and verify design predictions. The second goal of the investigation was to determine the suitability of the Special Test Section (STS) for development of cross-beam techniques and the conduction of routine cross-beam and fluctuating pressure experiments.

Verification of the design predictions and determination of operational procedures involved establishment of the following performance characteristics:

- Test zone Mach number variation with handcrank (dial) settings
- Distance between the end of the outerwall and downstream tip of the plug for the various Mach numbers (measured along the X-axis)

- Angular and radial Mach number distributions for fixed outerwall setting
- Steady state run time.

Relative suitability of the STS for cross-beam experiments and routine fluctuating pressure tests was investigated by determination of the following:

- Fluctuating pressures at various critical locations along the length of the test section
- Structural vibrations at points of interest in the test section
- Acoustic noise in the test cell (room containing test section).

These characteristics essentially constitute the static and dynamic calibrations of the test section. The static characteristics are important from a future operational point of view and dynamic characteristics are required for the purpose of establishing instrumentation requirements for future tests of separated base flows.

The remainder of this report discusses the following areas. Section II describes the static calibration studies including models and instrumentation. Section III gives the details of the dynamic calibration. The conclusions and recommendations are given in Section IV. A discussion of the facility and a pictorial review of the test setup are presented in the Appendix.

Section II

MACH NUMBER AND STEADY STATE CALIBRATION

2.1 OBJECTIVES

In order for the plug-nozzle special test section to be acceptable for cross-beam studies, various design predictions had to be verified. Model Mach number distribution across the flow annulus of the test section was required to have minimum deviations from nominal. Desired, nominal Mach numbers had to be attainable within close tolerances by external handcrank adjustments, and steady state run time of the tunnel had to be of a duration that would permit adequate data acquisition for cross-beam analysis.

The following test objectives were established to determine the preceding performance characteristics:

- Radial and angular distribution of Mach number across the test section annulus
- Nominal Mach number variation as a function of the gear-linked handcrank (this dictates outer-shroud position with respect to a fixed-plug and hence fixes distance between downstream end of plug and outer shroud)
- Steady run time that was acceptable for all models under consideration.

Prior to proceeding with a discussion of the results that satisfy the stated test objectives, Subsections 2.2, 2.3, and 2.4 present a brief examination of the special test section, the models, and discuss the instrumentation employed.

2.2 SPECIAL TEST SECTION

The special test section was designed to fit into MSFC's 14- by 14-Inch Transonic Wind Tunnel. The contours were generated by a method of characteristics solution using a boundary layer correction routine. The test section (Figures 2-1 and 2-2) is basically an axisymmetric plug-nozzle with an annulus flow section. Models are attached to the downstream portion of the plug.

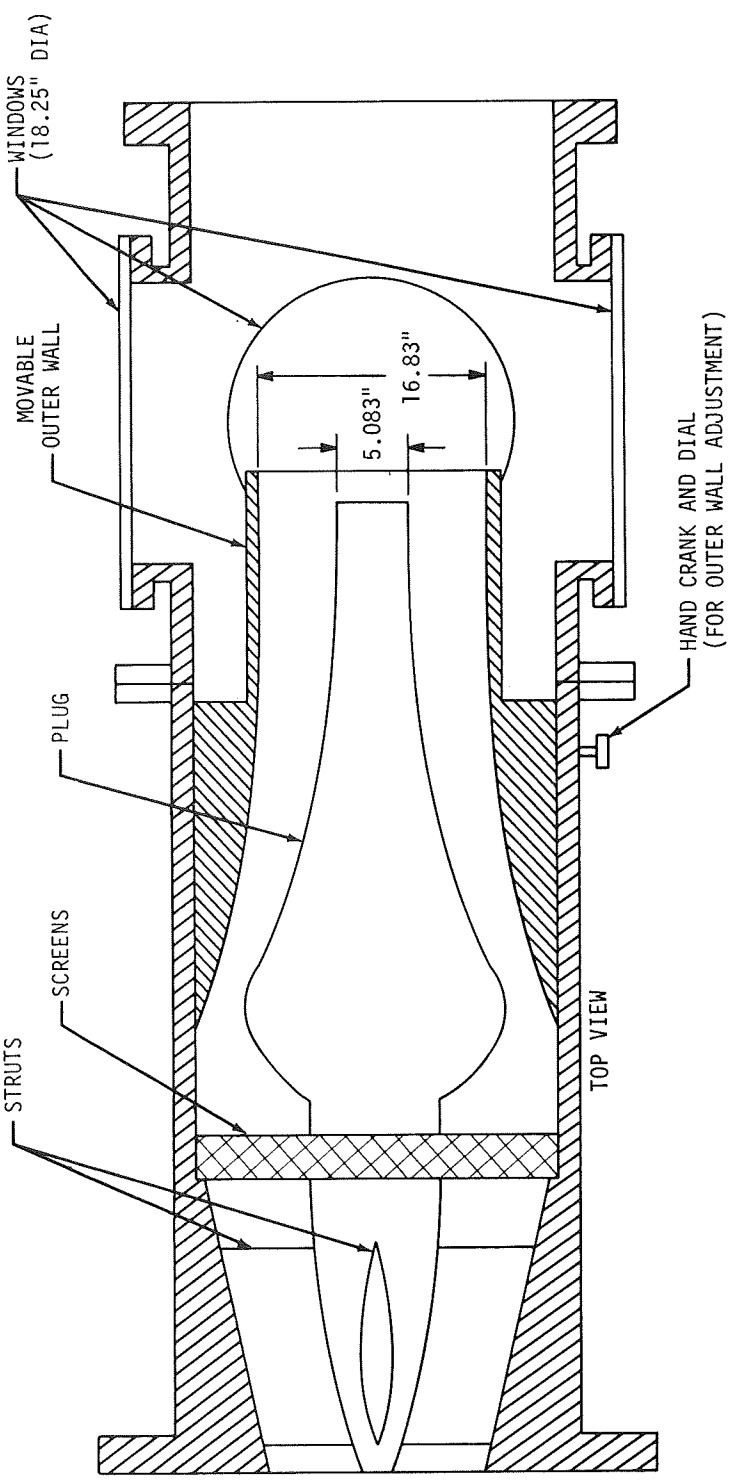

NOTE: THE OUTER WALL CAN BE EXTENDED BY 6" AND 10" PLEXIGLASS EXTENSIONS.

Figure 2-1. SCHEMATIC DETAILS OF MODIFIED SPECIAL TEST SECTION

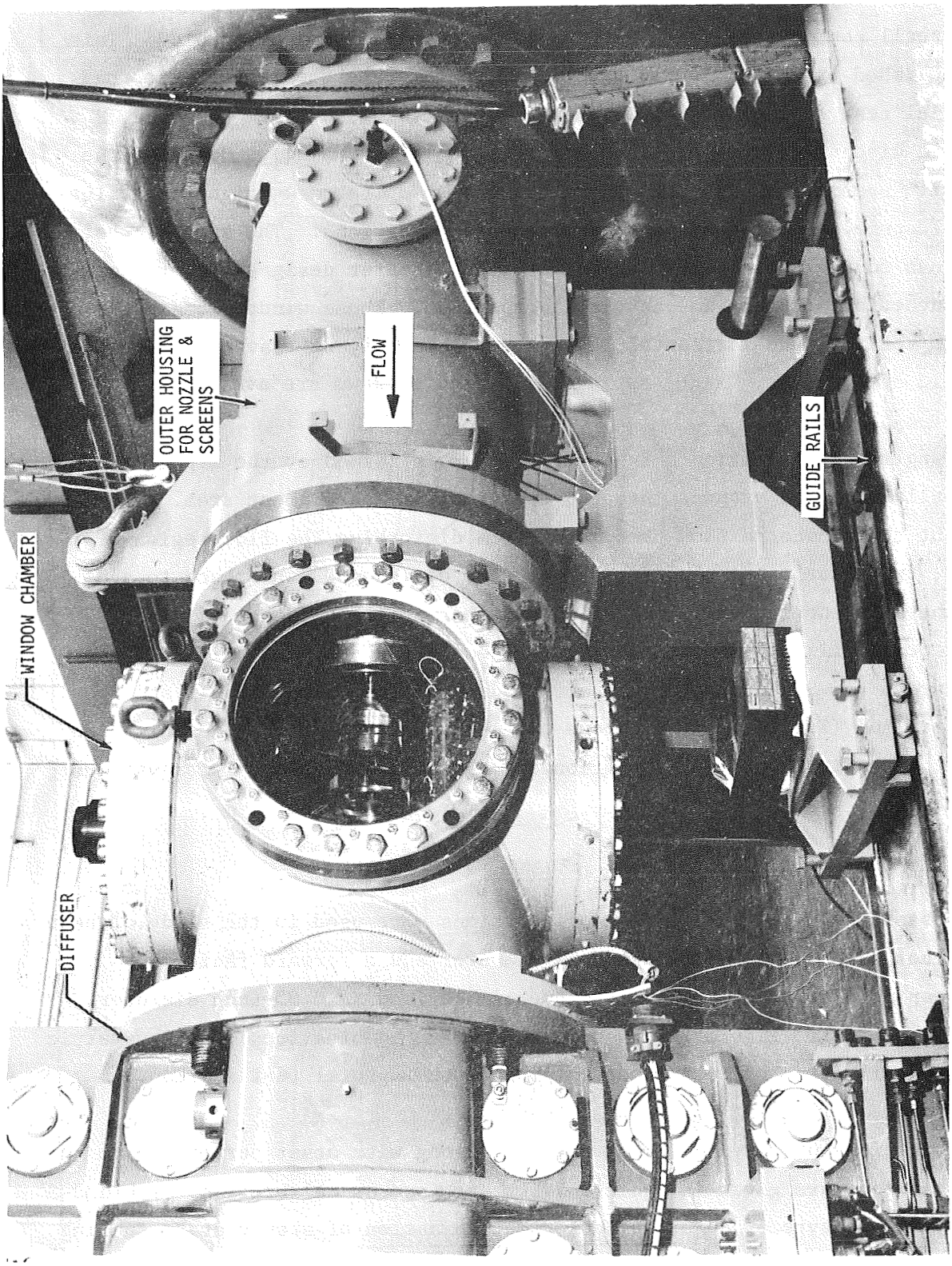

Figure 2-2. PICTORIAL VIEW OF THE MODIFIED SPECIAL TEST SECTION

Mach numbers vary from about 1.80 to 2.86 and are determined by movement of the outerwall contour (Figure 2-3) with respect to a fixed center-plug. This is accomplished by a gear-linked handcrank, operated by the tunnel personnel. The special test section was designed to be operated at a total pressure, P_o, of 30 psia discharged to vacuum conditions ($\approx$ 20 to 29 mm Hg). However, the tunnel with special test section installed can be operated at higher P_o values ($\approx$ 60 - 70 psia) and discharged to atmospheric conditions. The special test section has four glass windows 18.25 inches in diameter designed to transmit electromagnetic radiation in the visible spectrum. These windows can accommodate vertical and horizontal light beams which may be traversed over the flow field of interest. Also, optional infrared windows are available.

During tunnel operation a free-shear layer is formed at the lip of the outer-nozzle wall and extends into the test section measurement area. Thus, to prevent this unwanted flow phenomenon from disturbing the flow region of interest, two transparent plastic shrouds were designed which attach to and extend the outer-nozzle wall. These shrouds permit transmission of visible light, hence facilitate remote sensing by cross-beam instrumentation. These shrouds are 6 and 10 inches long to accommodate various sized models and model extension (Figure 2-3). Various model-extension combinations which can satisfy the condition of no interaction are depicted in Table 2-1 for various Mach numbers.

2.3 MODELS

Two basic axisymmetric model configurations were used in the study. These were a blunt base model 5.083 inches in diameter and a forward facing 90-degree step model with a 5.083-inch diameter body and an 8.95-inch diameter step. These models (Figure 2-4) were used in five combinations of axisymmetric extensions, all attached to the center plug of the special test section.

Combinations of model and Mach numbers, along with other pertinent run log information, are given in Table 2-2 for Mach number calibration. Table 2-3 depicts the same type of information for determination of steady state running

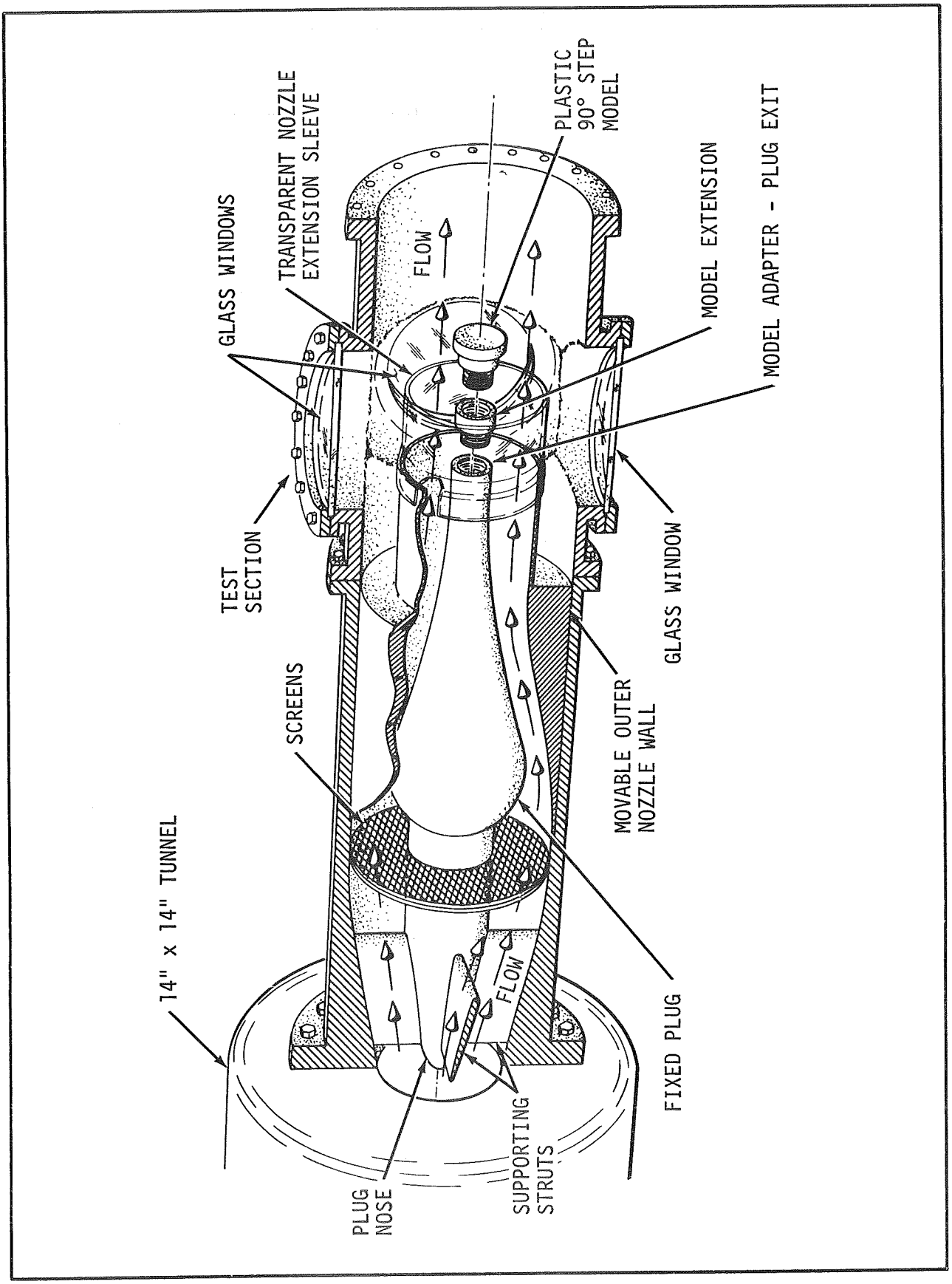

Figure 2-3. ASSEMBLY SKETCH OF MODEL AND SPECIAL TEST SECTION

Table 2-1. CONFIGURATIONS OF MODELS AND EXTENSION

These Satisfy the Condition of No Interaction of Either Lip Shock With The Model or Separation Shock With The Outerwall (or its Extension)

Mach No.	Model	Plug Extension Length in inches	Outerwall Extension Length in inches
2	90° step 8.75" long and 45° step	4.4	None
2	"	5.4	6
2.5	"	1.5	None
2.5	"	1.5	6
2.8	"	None	None
2.8	"	None	6
2	Base Flow	None	None
2	"	None	10
2	Boundary Layer Model 6.6" Long	5	None
2	"	5	6
2.5	"	1.9	None
2.5	"	1.9	6
2.8	"	None	None
2.8	"	None	6

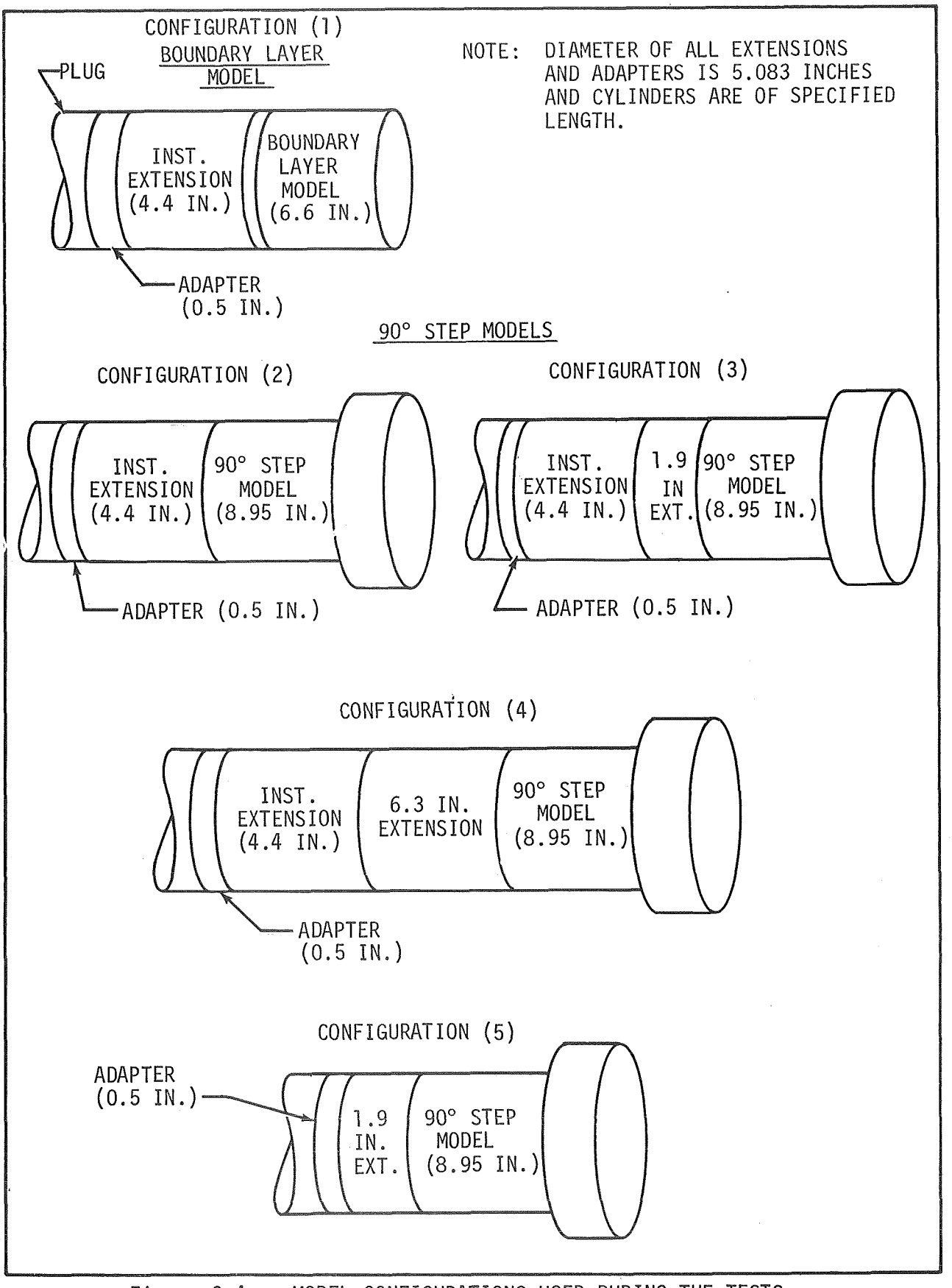

Figure 2-4. MODEL CONFIGURATIONS USED DURING THE TESTS

Table 2-2. RUN SCHEDULE FOR MACH NUMBER CALIBRATION TEST

Run No.	† Rake Angular Coordinates, Φ	Model Configuration	Mach No.	Counter Setting
1/4	0	1	2.8	3900
2	180	1	2.8	3900
3	180	1	2.5	2900
4	0	1	2.5	2900
5/2	0	1	2	1380
6	180	1	2	1380
7	45	1	2	1380
8	225	1	2	1380
9	90	1	2	1380
10	270	1	2	1380
*11/8	0	1	1.8	800
*12	180	1	1.8	800
**13	180	1	2	1380
14	Cancelled because - high pressure run			
15	180	1	2.8	3900
16	Cancelled due to lack of test time			
***17	180	1	2	1380

NOTES:

* Flow was not established during these runs.

** During this run the stagnation pressure (P_{op}) was raised from 35 psia to 60 psia with the hope that this procedure would lessen severe loads that result from starting at high pressures. This run also caused severe damage to the tygon tubing which resulted in cancellation of all high pressure runs.

*** This run was made with a 6-inch outerwall extension in order to determine the effect on calibration.

† Figure 2-5 shows the rake angular coordinate system (i.e., measurements of Φ)
(Note: Rake was always canted about 30 degrees to radius as it was rotated around the flow annulus.)

Table 2-3. RUN SCHEDULE FOR DETERMINATION OF STEADY STATE AND THE DYNAMIC CALIBRATION

Run No.	Tape No.	Nominal Mach No.	Schlieren	Model Configuration	Outerwall Extension	Remarks
†101/2	1	2	5000 frames/sec	1	6	
*102	1	2	"	"	"	Too short run duration
103	1	1.8	"	"	"	Flow not established
101	1	2.5	"	"	"	
105	1	2.8	"	"	"	
106	2	2.8	"	2	"	
107	2	2	"	2	"	
108	2	2	"	4	"	
109	2	2	64 frames/sec	4	"	
**110	2	2	"	1	"	ϕ = 0, TR7 & TR8 transducers face vertically upward
**111	2	2	"	1	"	ϕ = -15°
**112	2	2	"	1	"	ϕ = -30°
**113	2	2	"	1	"	ϕ = -45°
†114/1	2	2	64 frames/sec	1	None	
†115/1	2	2	"	3	6"	
116	3	2	"	5	6"	TR. #5, 6, 7, 8, 12, 15, 20, 21, Ax and Ay disconnected
117	3	2	"	2	6"	
118	2	2.5	"	1	6"	No dynamic data. Tape recorder malfunction

Notes:

* High pressure run 45, psia

** During these runs angular variation of the dynamic flow characteristics were measured.

† The slash numbers indicate the number of additional attempts made to acquire acceptable data.

time. The technique used for determination of the test time did not permit the presence of the rake in the flow, thus runs shown in Table 2-1 could not be used for this purpose. The dynamic data discussed in a later section were also obtained during these runs.

During the Mach number calibration phase of the tests, Model Configuration No. 1 (Figure 2-4) was used exclusively; however, during the phase of the tests devoted to the determination of the duration of the useful test time, all configurations 1 through 5, (Figure 2-4) were used.

It should be pointed out here that models other than those discussed in this report are available, and, in the pretest memorandum (ref. 1), plans were formulated to test some of these models at different Mach numbers. Some of these runs were deleted to save time and expedite acquisition of the enclosed data. The models that are available are listed in Table 2-4.

2.4 INSTRUMENTATION

The Mach number was obtained from the measurements of static and total pressures of the flow. Two rakes, one consisting of static probes, the other of total probes (eleven each), were positioned to measure the pressures one-inch downstream of the exit plane of the outerwall. The rake probes were numbered as P_{RS}^{1}, P_{RS}^{2}, ..., P_{RS}^{11}, and P_{RT}^{1}, P_{RT}^{2}, ..., P_{RT}^{11}. The rakes were too large to be accommodated along a radius. Hence, they were canted 30 degrees from the radius. Figures 2-5 and A5 show the details of the rakes and the manner in which they were mounted. The rake assembly was rotated about the tunnel axis to cover a range of angular positions including 0°, 45°, 90°, 180°, 225° and 270°.

One total pressure probe, P_o, was located in the settling chamber and another P_{op}, was located on the plug downstream of the screen assembly. Additionally, one static-pressure port, P_S, was located on the outerwall approximately two inches upstream of the exit plane (Appendix, Figure A-2). These pressures were used for the calculation of the nozzle Mach number and total

Table 2-4. MODELS AVAILABLE FOR THE SPECIAL TEST SECTION

I Jet Cluster Model - 415 (Assy Drawing No. 80M51029)

II Metallic Plug adapter (Drawing No. 80M42112)

III Metallic Plug extensions

Length in Inches	MSFC Drawing No.
1.5	80M31934
1.9	80M31935
4.4	80M42180
5.0	80M42115
5.4	80M42109
6.3	80M42110
8.4	80M42116
10.3	80M42111

IV Noses of various types, made out of Plexiglas

Type	Length in Inches	MSFC Drawing No.
Cylinder	6.6	80M32195
90° Step	6.7	80M31936
45° Step	6.7	80M32194
45° Protu-berance	8.95	80M42114
45° Protu-berance	11.2	80M42113

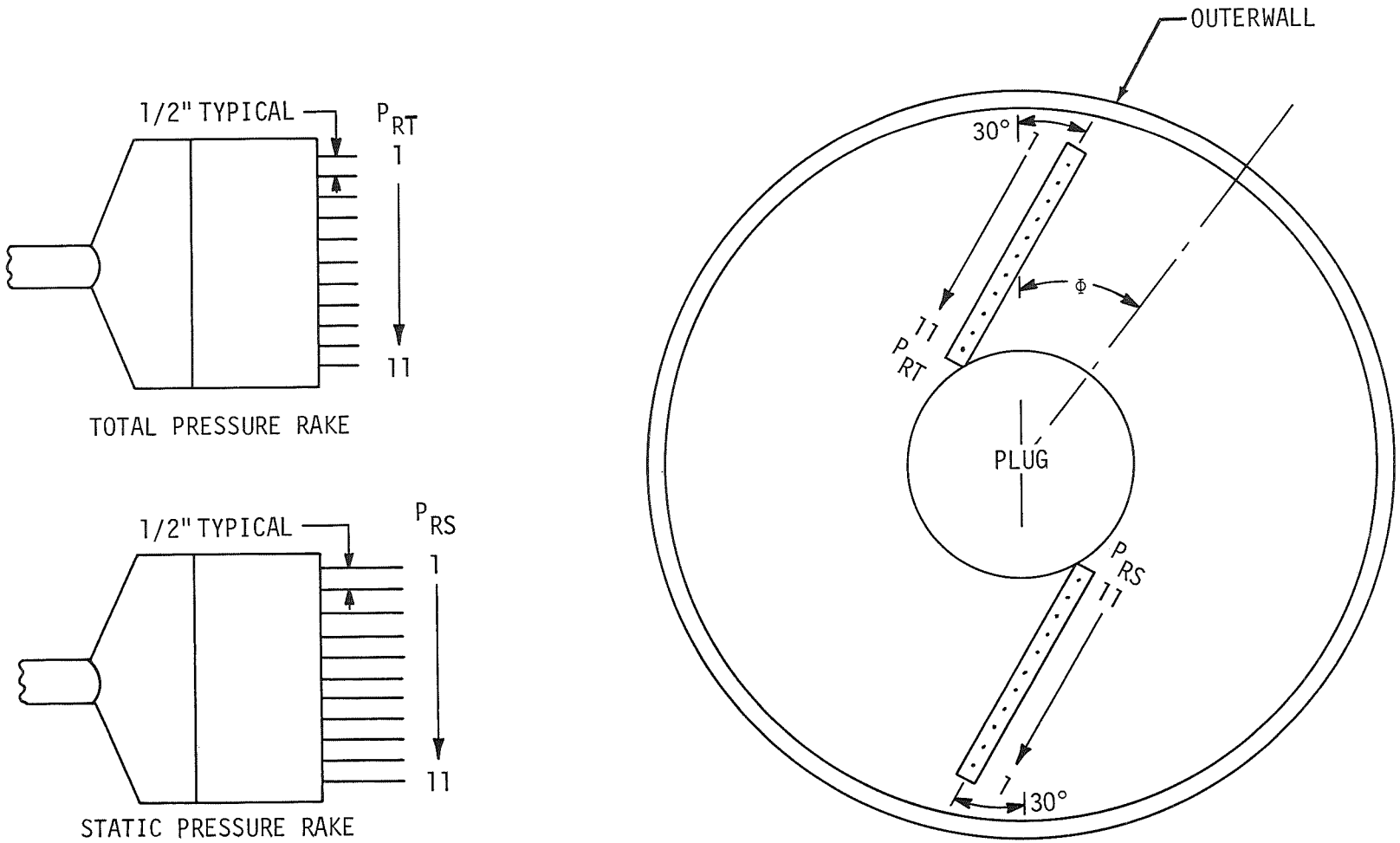

NOTE: Φ POSITIONS USED FOR MEASUREMENT OF AZIMUTHAL VARIATION OF MACH NUMBER WERE 0°, 45°, 90°, 180°, 225° AND 270°.

Figure 2-5. STATIC AND TOTAL PRESSURE RAKES AND THEIR ORIENTATION IN THE TEST SECTION

probe local Mach numbers. A bar with nine pressure ports, 0-1 through 0-9, was located in the window cavity. Figures 2-6 and A-9 show the locations of the pressure ports described above.

A Schlieren movie system which was capable of providing time-reference marks was used to obtain optical coverage (at 60 frames/sec) of the flow field. The pressures 0-1 through 0-9 and the Schlieren movies were taken to provide information on the duration of the test time; however, the movies were of little value because of poor quality.

All pressure probes and ports were connected to a Scannivalve System by use of tygon tubing, which was used essentially for providing a flexible length required for the different settings of the outerwall for various Mach numbers. Data were sensed here by a strain gauge transducer, fed to an Endevco signal conditioning module, then directed to the Systems Engineering Laboratory (SEL) digital data acquisition system, and finally recorded on Hollernth (punch) cards (Figure 2-7). The data were then reduced by a general purpose digital computer.

2.5 DATA REDUCTION

To facilitate the measurement of static and total pressure at all 22 probe locations, the rake assembly was rotated by 180 degrees about the tunnel axis between the consecutive runs for a given outerwall setting. From these measurements the rake Mach number, M_R, was calculated using the Rayleigh-Pitot relation (ref. 2) for air as shown below

$$\frac{P_{RTi}}{P_{RSi}} = \left[\frac{6M_{Ri}^2}{5}\right]^{7/2} \left[\frac{6}{7M_{Ri}^2 - 1}\right]^{5/2} \qquad (1)$$

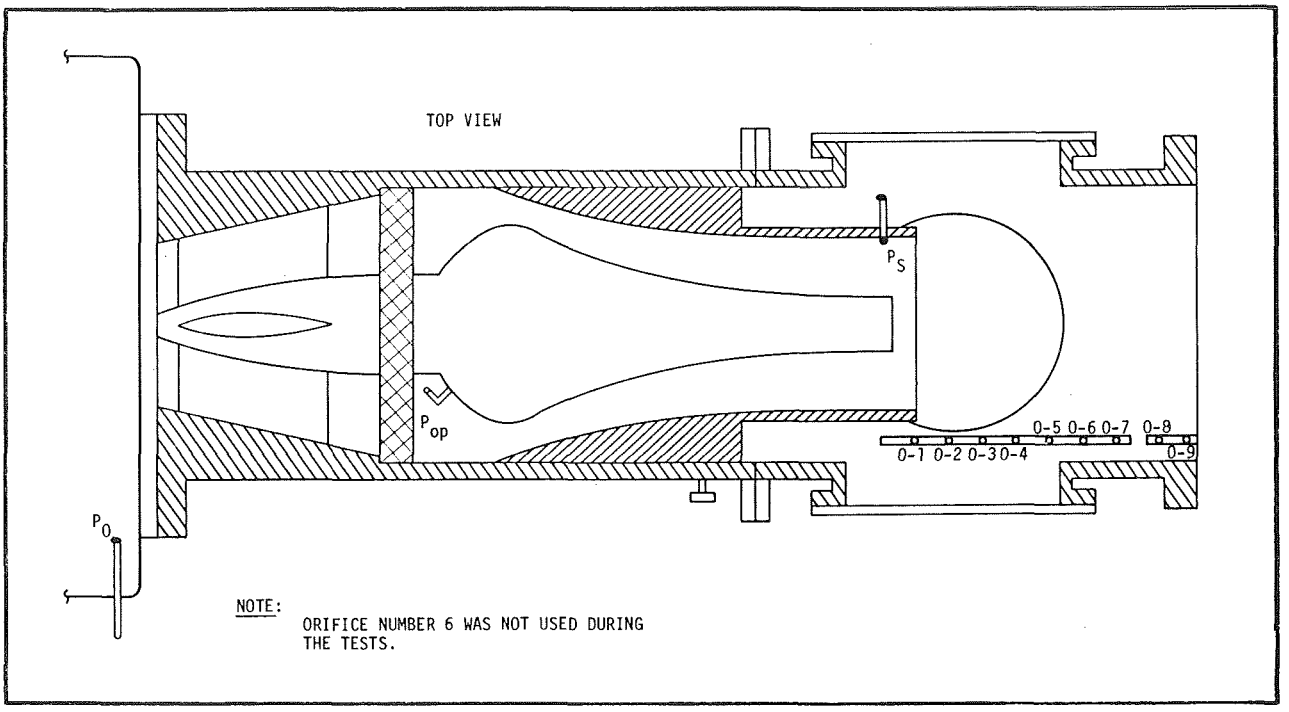

Figure 2-6. AXIAL LOCATIONS OF PRESSURE ORIFICES

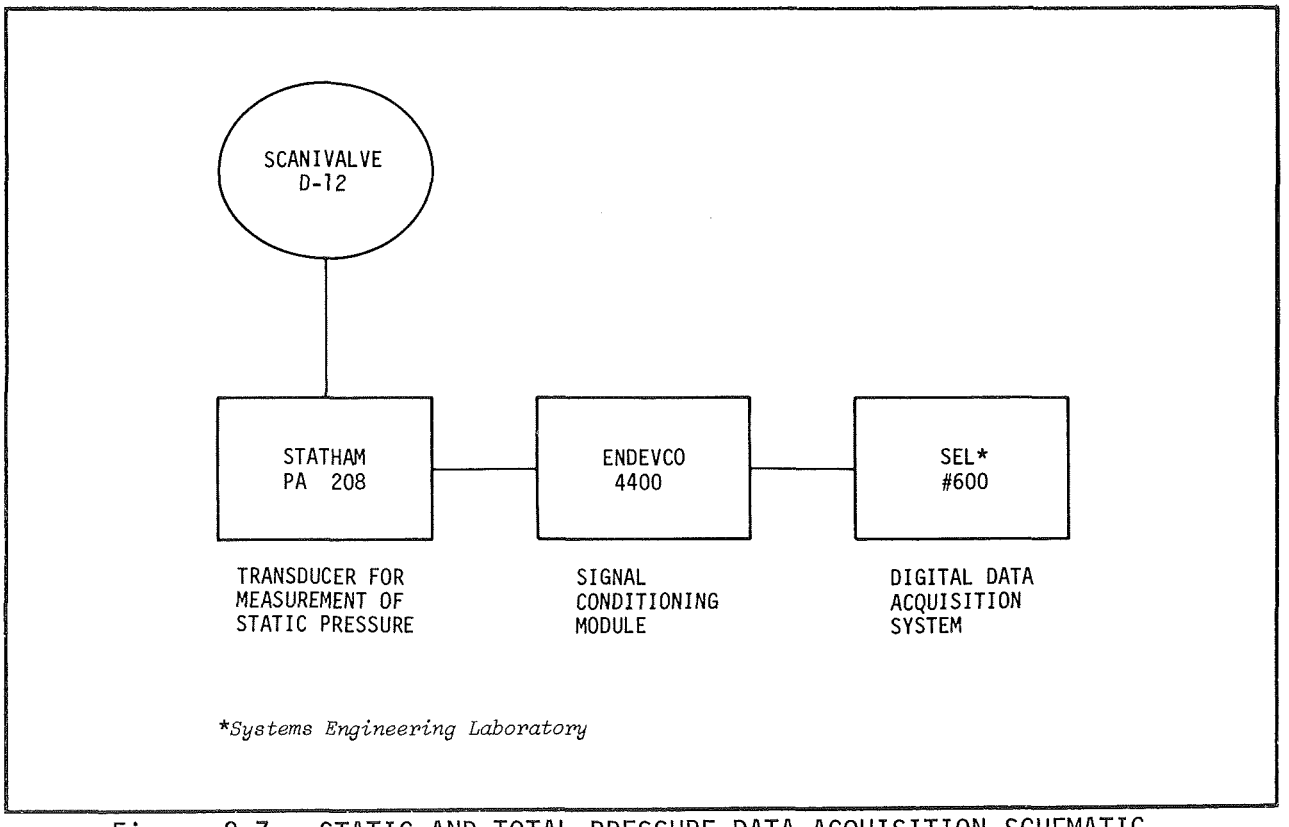

Figure 2-7. STATIC AND TOTAL PRESSURE DATA ACQUISITION SCHEMATIC

where P_{RT} and P_{RS} are the total and static pressure, i indicates the position of the probes and M_{Ri} is the rake Mach number at the location of the probes. It should be noted that the pressures P_{RTi} and P_{RSi} for a given location, i, are measured during two consecutive runs, and the deviations of the control pressure during these runs can affect the results considerably. Only a representative set of data were analyzed using this approach (see Section 2.6.4).

If one assumes the upstream-total pressure as equal to the measured plug pressure, P_{o_p}, then one may use the one-dimensional normal-shock relation to obtain local Mach numbers, M_L, at the locations of the total pressure tubes. This gives the following relation for the Mach number M_L.

$$\frac{P_{RTi}}{P_{o_p}} = \left[\frac{6M_{Li}^2}{M_{Li}^2+5}\right]^{7/2} \left[\frac{6}{7M_{Li}^2-1}\right]^{5/2} \qquad (2)$$

The nominal nozzle Mach number, M_N, can then be calculated by using the static pressure measured at the location P_S and the plug total pressure P_{op}, by the use of the following one-dimensional isentropic-flow relation (ref. 2).

$$M = \sqrt{5\left[\left(\frac{P_S}{P_{o_p}}\right)^{-2/7} - 1\right]} \qquad (3)$$

For measurement of the duration of useful test time the static pressure in the window cavity was measured every second from the start to the end of a given run. The portion of the test time that does not include the flow accelerations at the start and the flow decelerations at the end of the tunnel run is the useful test time during which the mean flow conditions are stationary. This is indicated on the pressure versus time curve by a horizontal line. The pressure orifice chosen for a particular run is the one near the exit plane of the outerwall.

The experiments (calibration and test time) were originally planned to cover a range of settling chamber pressures from 30 psia to 60 psia; however, tygon tubing-rupture presented a severe problem at pressure levels beyond 35 psia. It was therefore necessary to discard all data for runs made at pressures greater than 35 psia because of tygon tube leakage.

2.6 MACH NUMBER CALIBRATION

2.6.1 Nozzle Nominal Mach Number, M_N and The Counter Setting "C"

Figure 2-8 gives the handcrank dial counter setting, "C", which indicates the positioning of the outerwall as a function of the nominal Mach number. The curve is apparently linear within the range of the test section Mach numbers investigated. Comparison of average experimental Mach numbers (one inch downstream of outerwall exit plane) to values computed by several method of characteristics solutions at various off-design positions is shown in figure 2-9. In general, good agreement is indicated, but small discrepancies could occur because a constant boundary layer correction was used for all calculated cases.

The operational range of the test section was found to be

$$1.97 \leq M_N \leq 2.78 \text{ or } 1380 \leq C \leq 3900.$$

The handcrank counter reading is controlled by a gear-linked mechanism. To insure that slack or a damaged gear did not result in variable counter readings with successive repeats of Mach number, several traverses were made. The run sequence (Table 2-3) was chosen to evaluate this effect, and during 1-1/2 cycles of traverse no discernable changes in the Mach number were observed for a given counter setting.

2.6.2 Nominal Mach Number and the Distance "d" Between the Downstream Ends of the Plug and Outerwall

This relation is required for the design of the models. Figure 2-10 gives the variation of "d" with M_N. This function is also linear in the range of the test section operation studied.

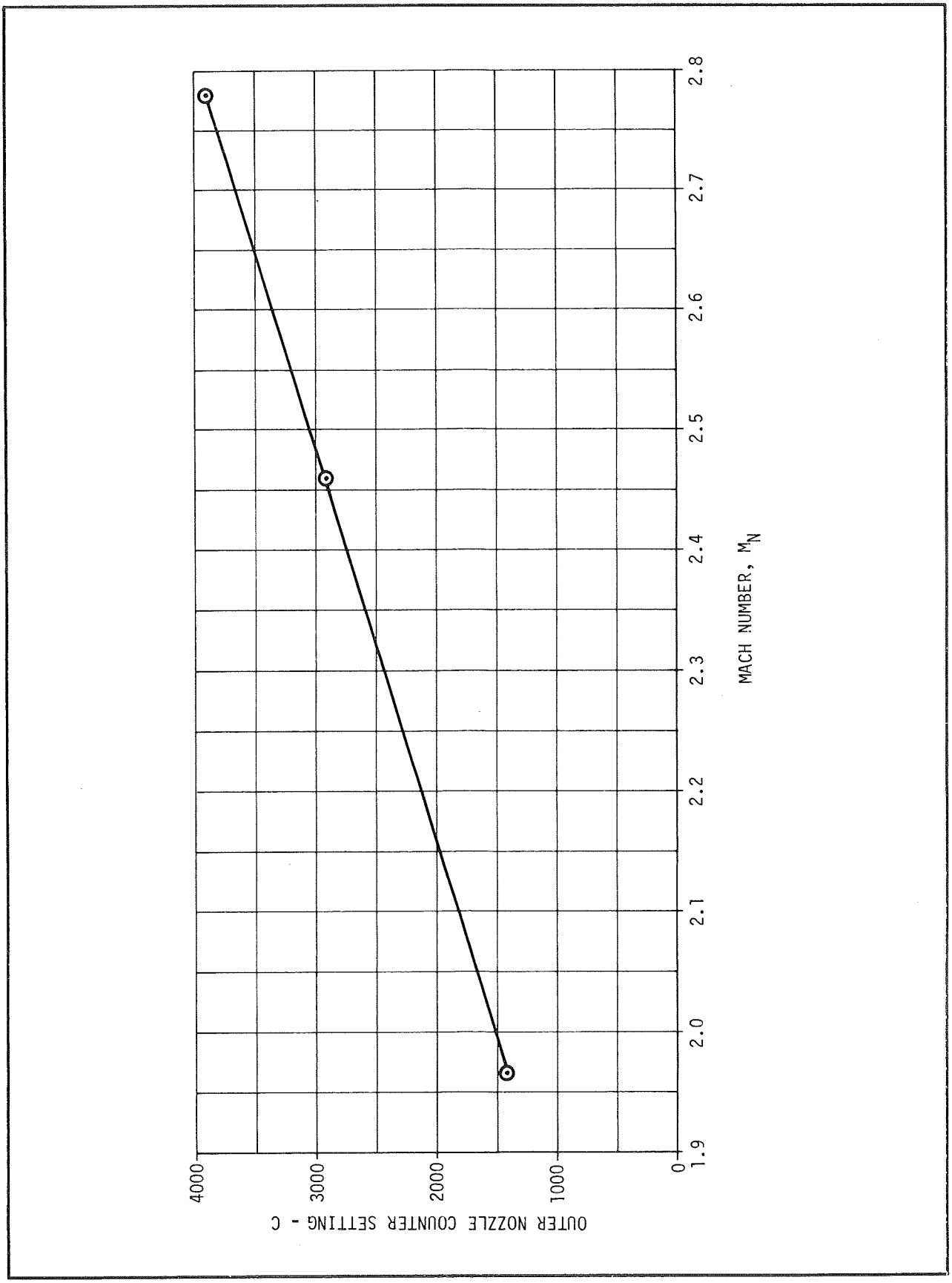

Figure 2-8. NOZZLE CALIBRATION - VARIATION OF OUTER NOZZLE COUNTER SETTING WITH MACH NUMBER

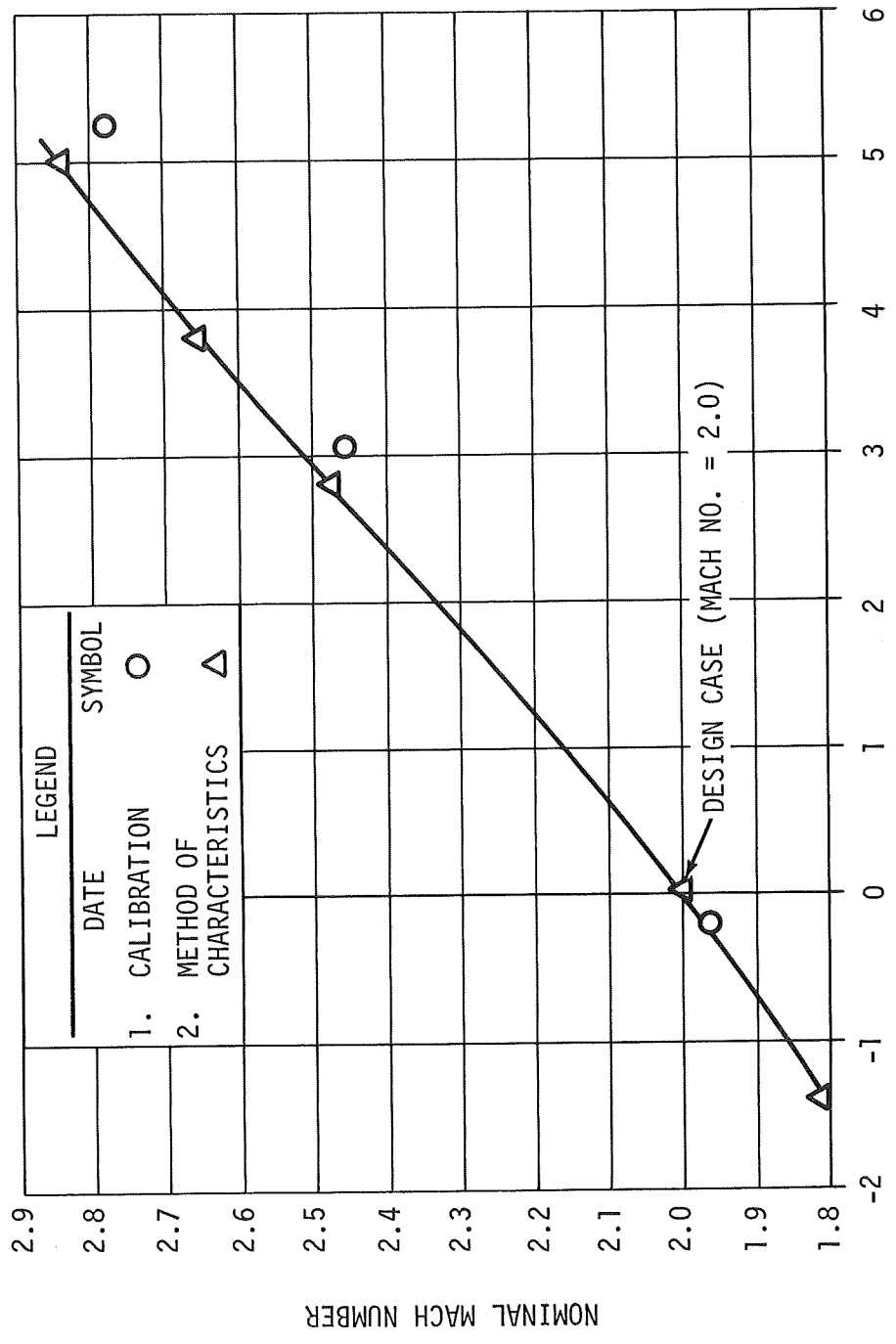

Figure 2-9. COMPARISON OF EXPERIMENTAL MACH NUMBERS TO METHOD OF CHARACTERISTICS SOLUTIONS

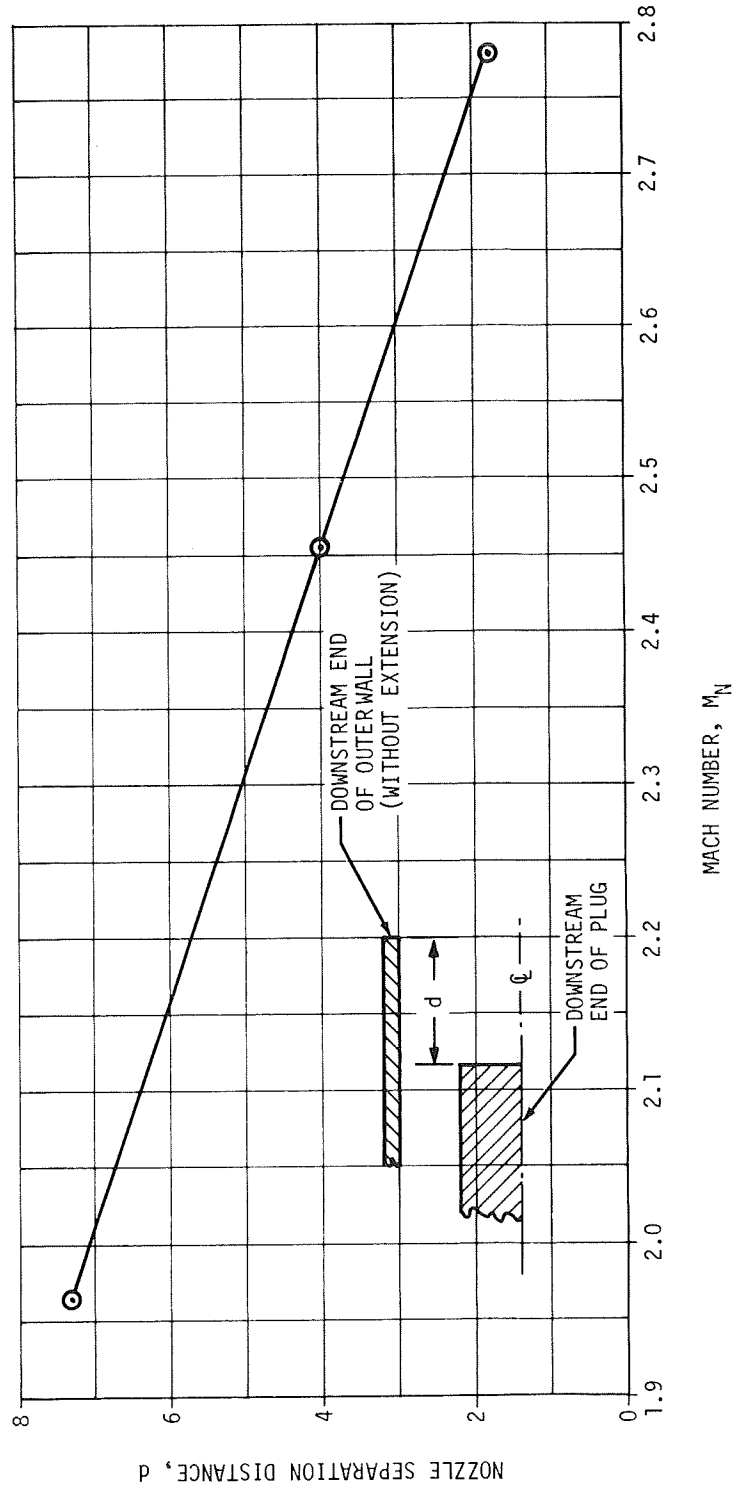

Figure 2-10. NOZZLE CALIBRATION-VARIATION OF NOZZLE SEPARATION DISTANCE WITH MACH NUMBER

2.6.3 Radial and Angular Variation of Local Mach Number, M_L

Figures 2-11, 2-12, and 2-13 illustrate the angular and radial deviation of local Mach number for nominal Mach number settings of 1.96, 2.48, and 2.82 at various axial positions (always one inch downstream of the outerwall exit plane). These outerwall positions correspond to respective "d" (distance between outerwall and end of fixed plug) values of 7.25, 4.0 and 1.8 inches. Reduction techniques used for these data are discussed in subsection 2.5

Complete radial measurements were taken (Figure 2-11) for operation of the STS in the vicinity of the design Mach number (M = 2) only. For these data, variation of Mach number was found to be on the order of 0.05. For purposes of comparison, design Mach number calculated by a method of characteristics solution varied less than .003 across the flow annulus. However, the calculated values correspond to an exit plane extending from the plug end to the nozzle lip. Data for the other cases (Figures 2-12, and 2-13) were taken only along the vertical axis at 0, and 180 degrees. These cases show a Mach numbers variation of 0.03 to 0.04.

It should be noted that these data are plotted on an expanded scale, hence, scatter is not excessive and is quite permissible since all points fall within range of instrumentation error. Thus, it may be concluded that there are no discontinuities in the test section which could result in nonuniformities in the flow. The special test section should, therefore, be acceptable for a wide range of static and dynamic testing.

2.6.4 Radial and Angular Variation of Rake Mach Number, M_R

Static pressure runs were reduced using methods presented in subsection 2.5. Some data from these probes were discarded for the following reasons:

- Tube leakage (as found by post-run pressure checks)
- Interaction of lip shock with probe
- Pinched tube.

Results from selected static data (Figure 2-14) indicate a Mach number variation of less than 0.04 across the annular region one-inch downstream of the nozzle exit. However, data from static rake probes generally had much larger deviations because of the reasons discussed above as well as inherent

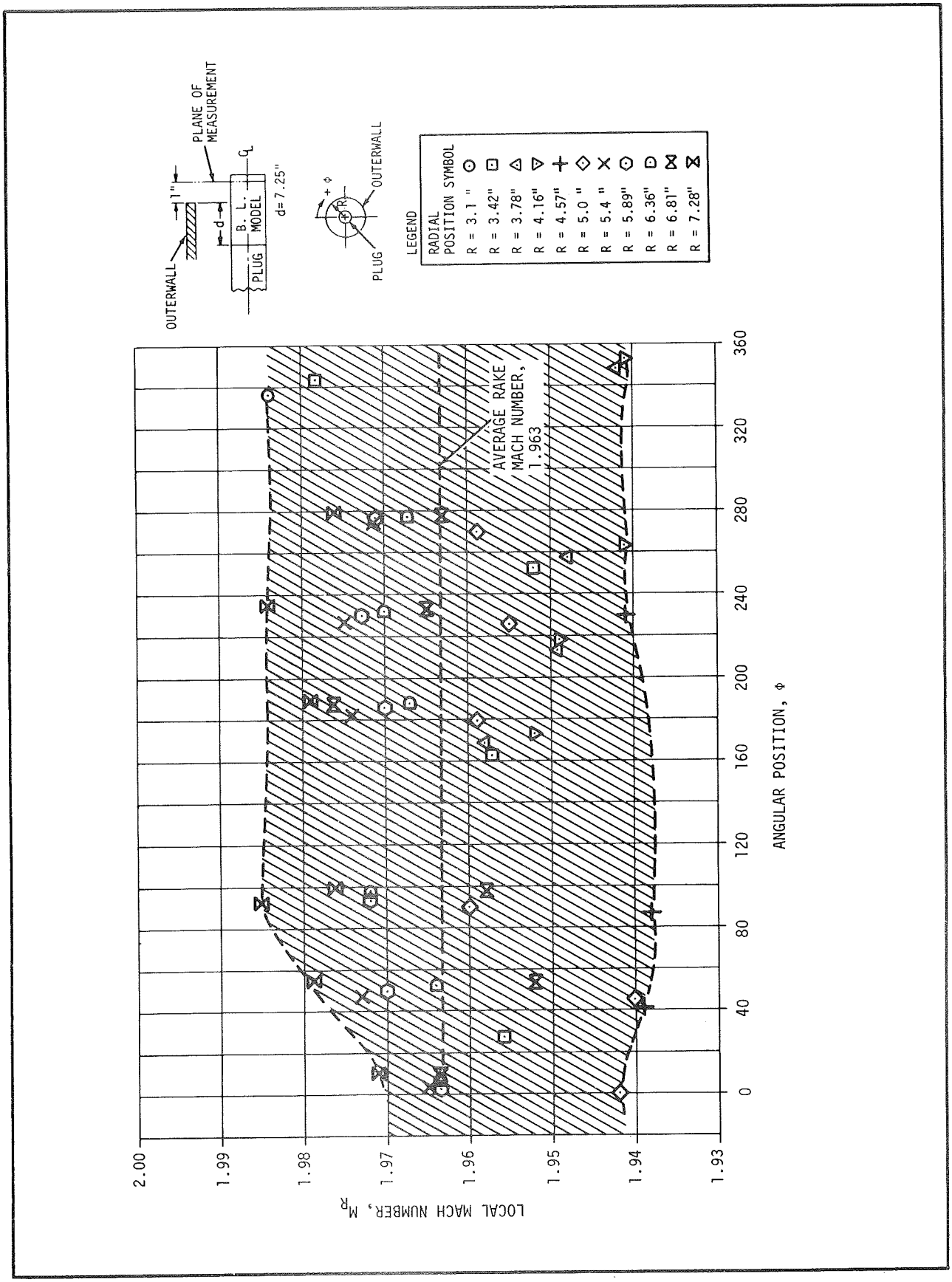

Figure 2-11. VARIATION OF LOCAL MACH NUMBER WITH ANGULAR POSITION, NOMINAL MACH NUMBER $M_N = 1.96$

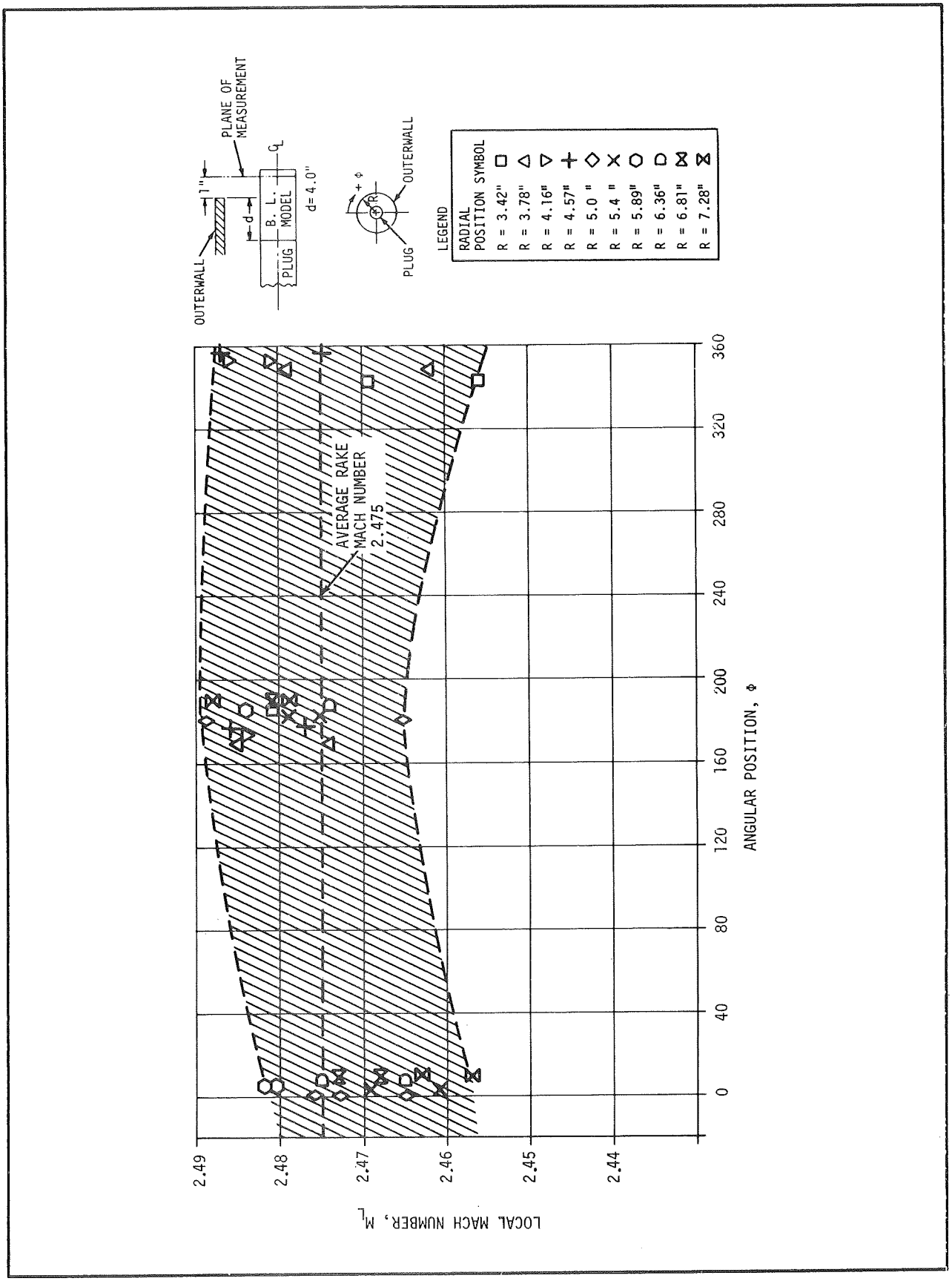

Figure 2-12. VARIATION OF LOCAL MACH NUMBER WITH ANGULAR POSITION, NOMINAL MACH NUMBER M_N = 2.48

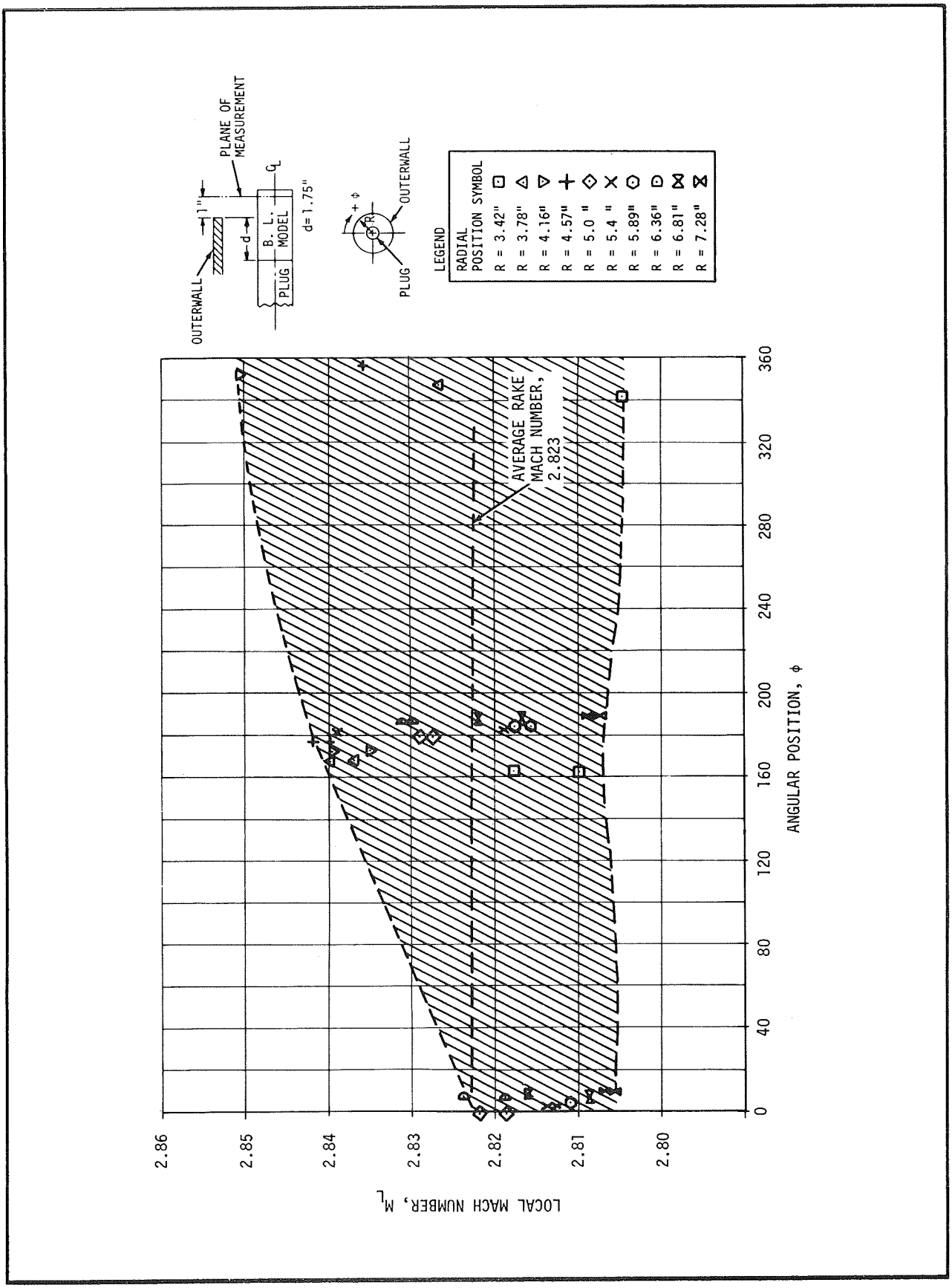

Figure 2-13. VARIATION OF LOCAL MACH NUMBER WITH ANGULAR POSITION, NOMINAL MACH NUMBER M_N = 2.82

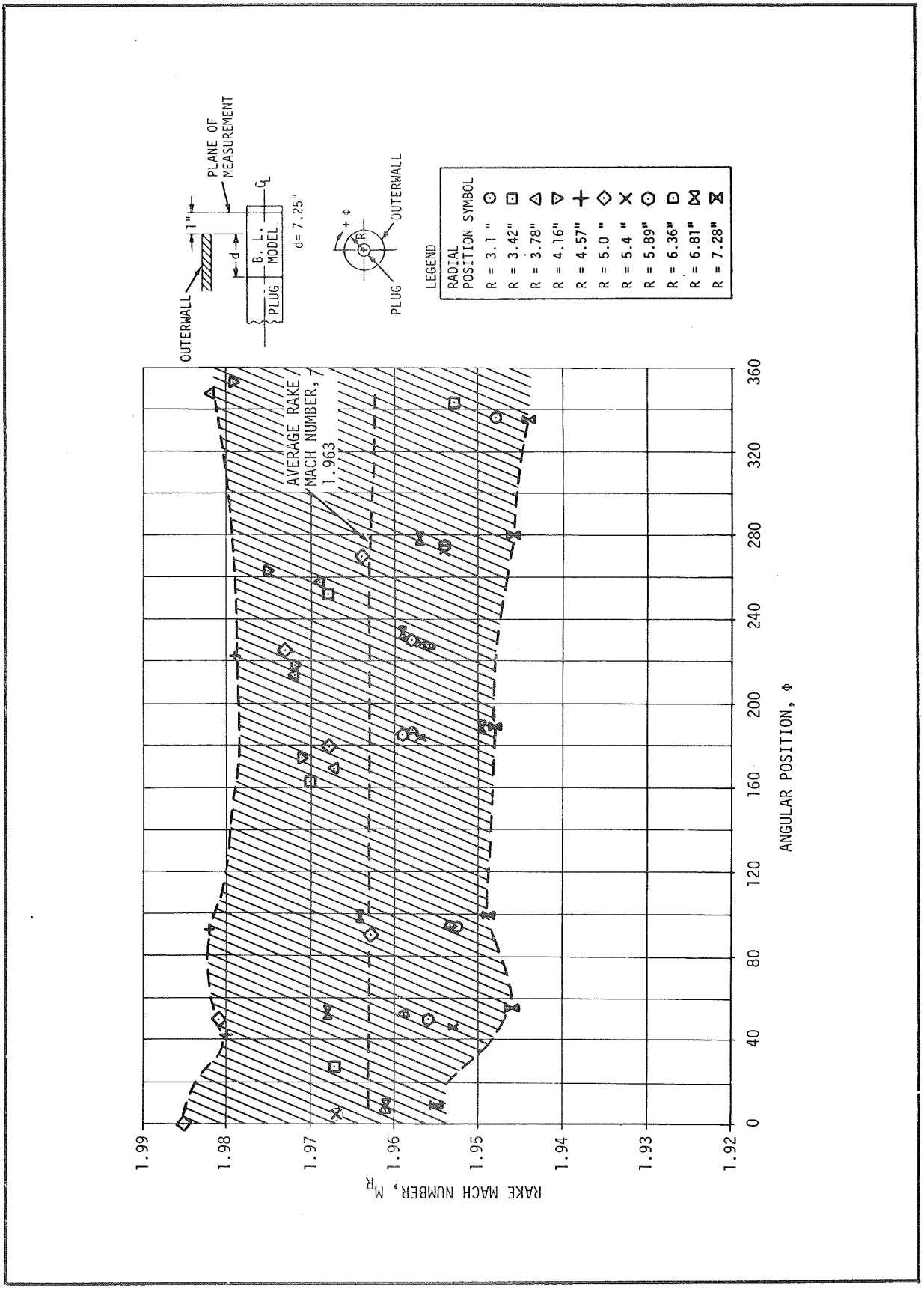

Figure 2-14. VARIATION OF RAKE MACH NUMBER CALCULATED WITH THE $\frac{P_{RTi}}{P_{RSi}}$ RATIO AS A FUNCTION OF ANGULAR POSITION, NOMINAL MACH NUMBER N_N = 1.96

difficulties associated with measurement of static pressures in supersonic streams. Hence, the static rake system was of limited use for calibration purposes.

2.7 DURATION OF STATIONARY FLOW

It was necessary to obtain dynamic data during that portion of a run for which the mean flow remained steady. It was anticipated that upstream or downstream conditions responsible for unsteadiness in the mean flow would be manifested in the variations of the wall pressures in the window cavity. Hence, the static pressure, P_E, in the window cavity was measured at the exit plane of the nozzle and various other locations. To insure that stream conditions were not dependent on model configuration (e.g., as a result of flow blockage), measurements were made with both boundary-layer and step-flow models. Figures 2-15 and 2-16 give the variation of P_E with time, respectively, for boundary-layer and 90 degree-step models. The outerwall extension (Figure 2-15) had essentially negligible effect on the time history of the mean flow in the case of the boundary-layer model. The 90-degree-step model was always tested with the 6-inch outerwall extension. In these figures, zero on the time axis corresponds to the time at which the operator presses the start button. Steady state conditions start after about 6 seconds and end approximately 24 seconds after the operator presses the start button. There is a slight increase in the duration of steady state run time with increasing nominal Mach number; however, model configuration has little effect.

It was also desired to establish the degree of steadiness of the mean flow in the nozzle. For this purpose the ratio P_E/P_S was used (Figures 2-17 and 2-18). Here P_E is the static pressure in the window cavity at the outerwall-exit plane and P_S is the static pressure on the outerwall, measured 2 inches upstream of the exit plane. Based on this ratio, the flow was stationary during usable run time. It may, therefore, be concluded that the shock oscillations associated with the nozzle-lip shock do not affect stationarity of the mean flow either inside or outside the nozzle for steady state duration.

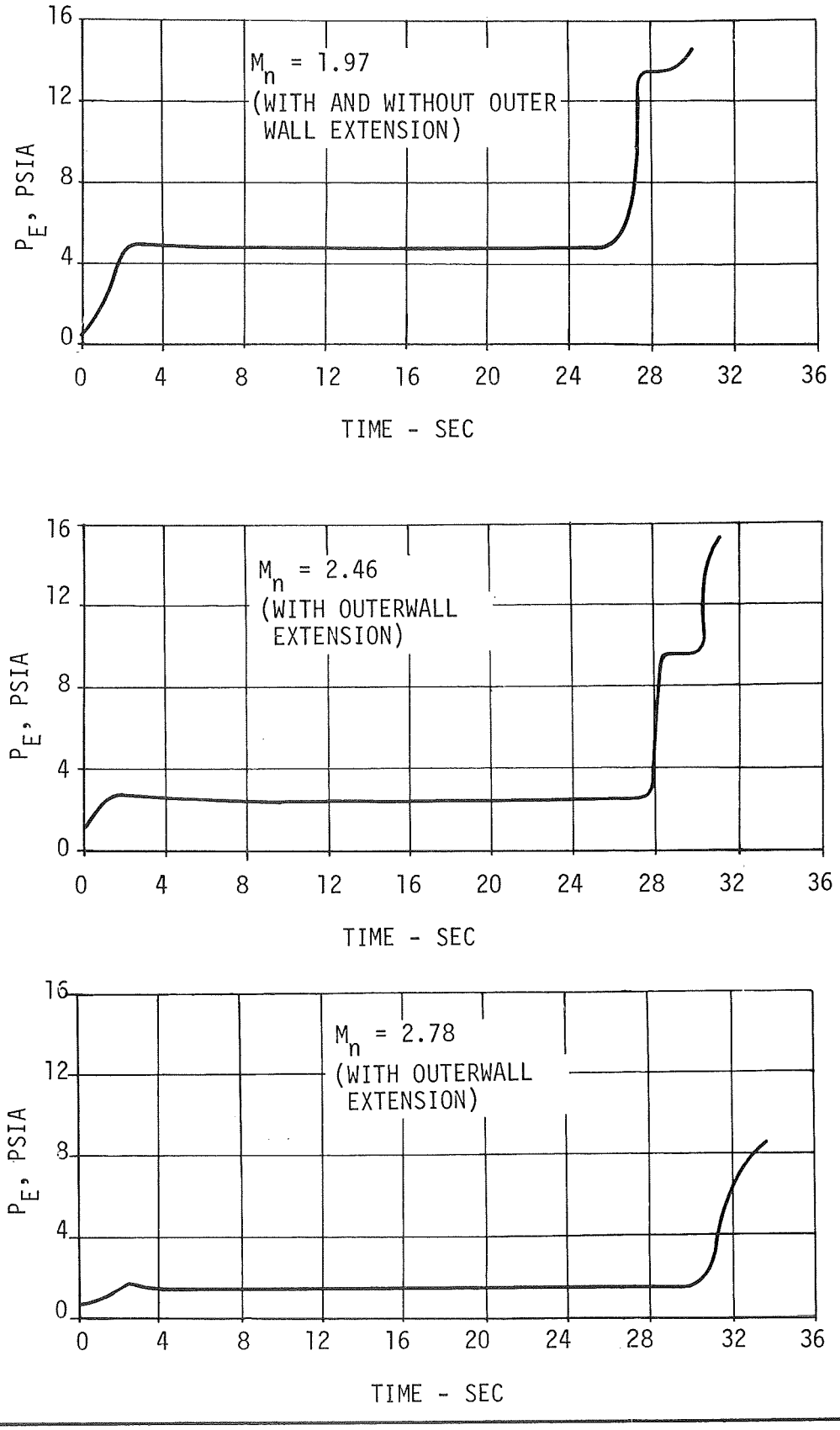

Figure 2-15. VARIATION OF P_E WITH TIME FOR BOUNDARY LAYER MODEL

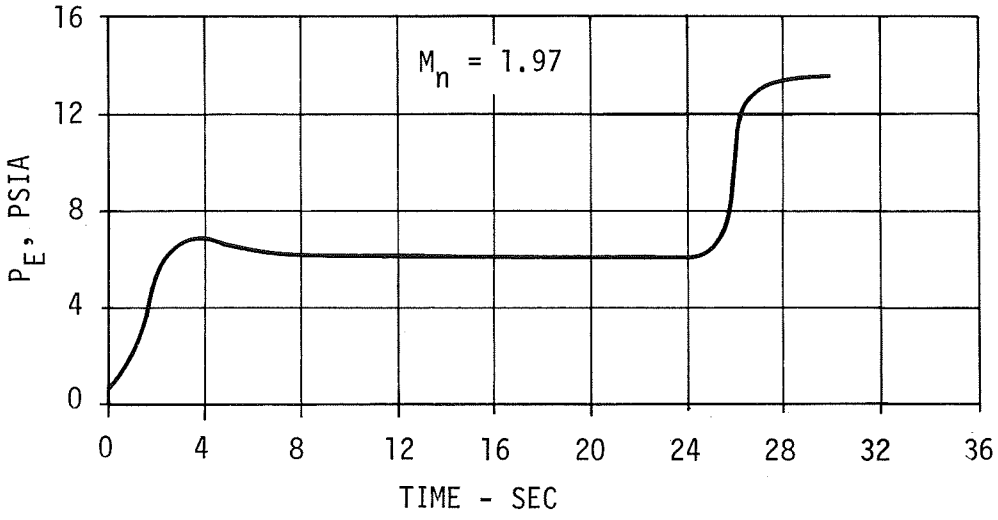

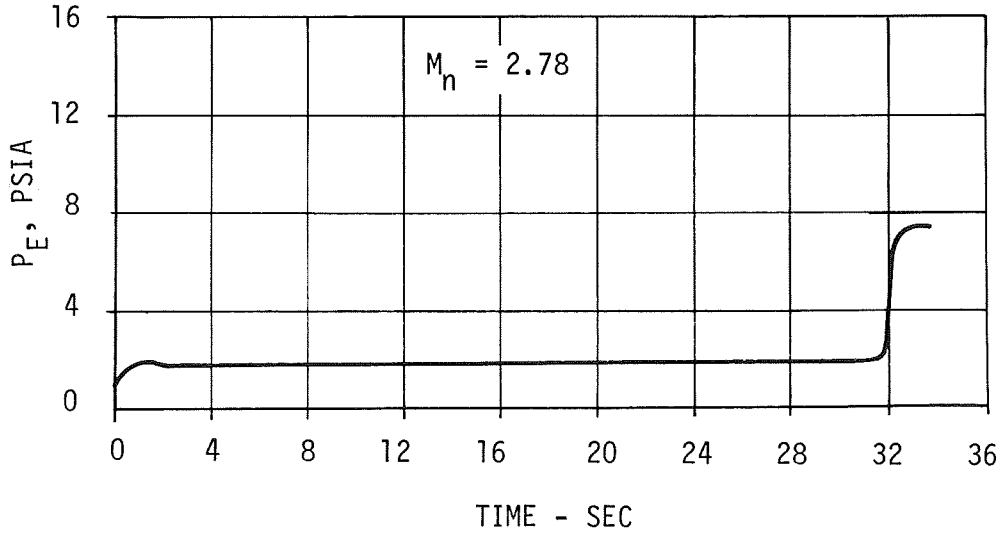

Figure 2-16. VARIATION OF P_E WITH TIME FOR 90° STEP MODEL (WITH OUTERWALL EXTENSION)

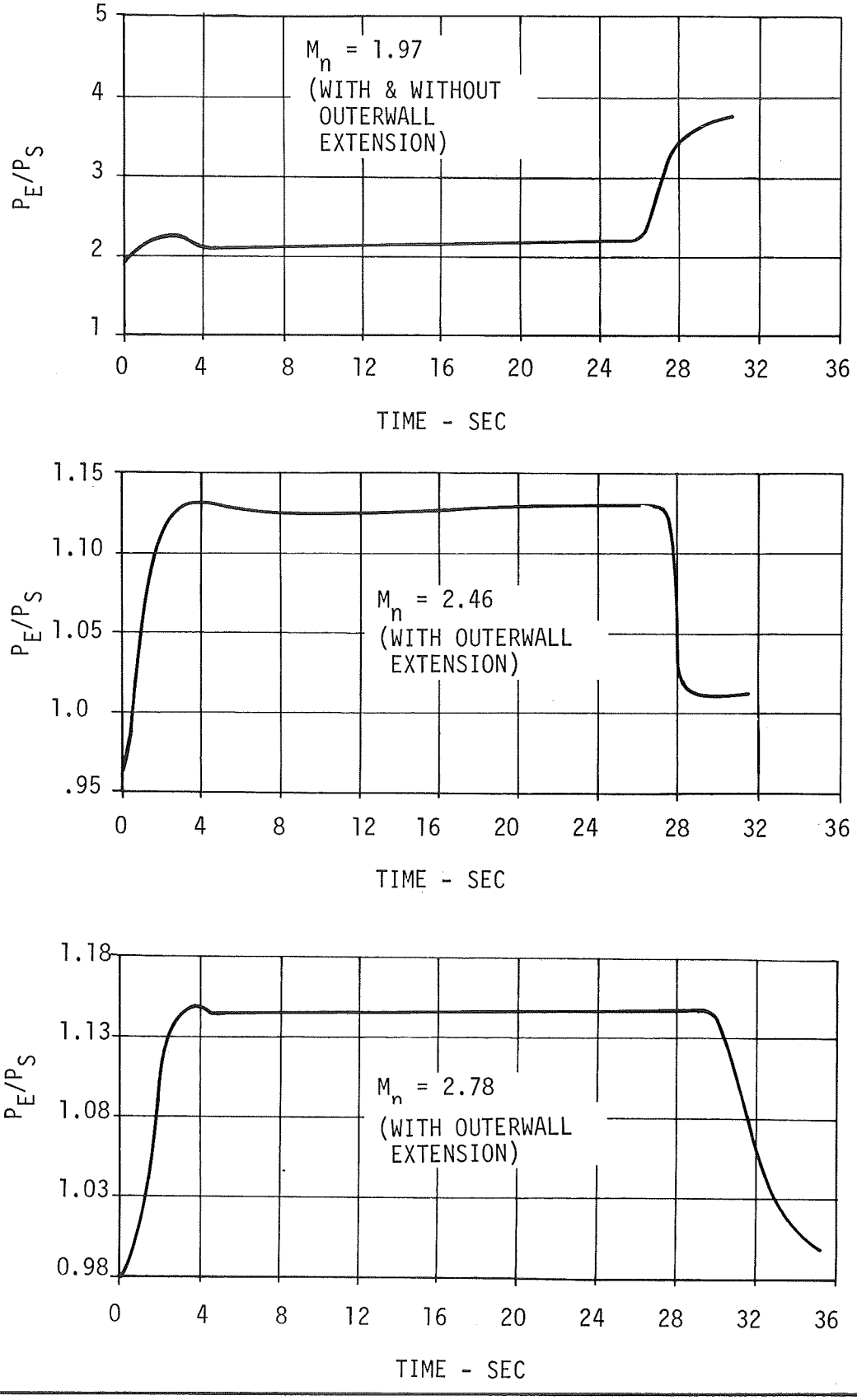

Figure 2-17. VARIATION OF P_E/P_S WITH TIME FOR BOUNDARY LAYER MODEL

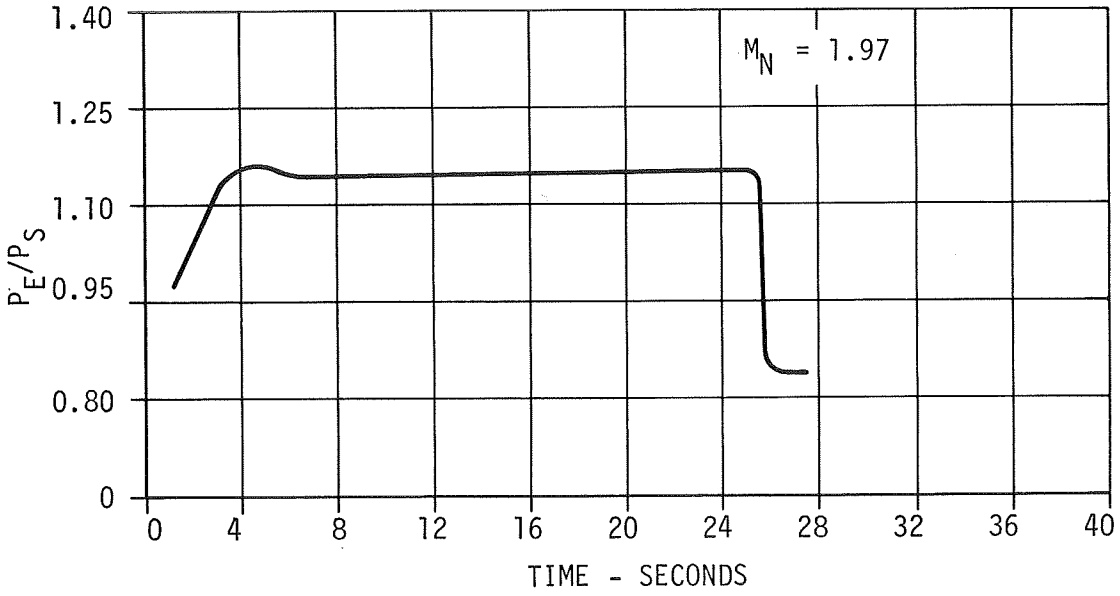

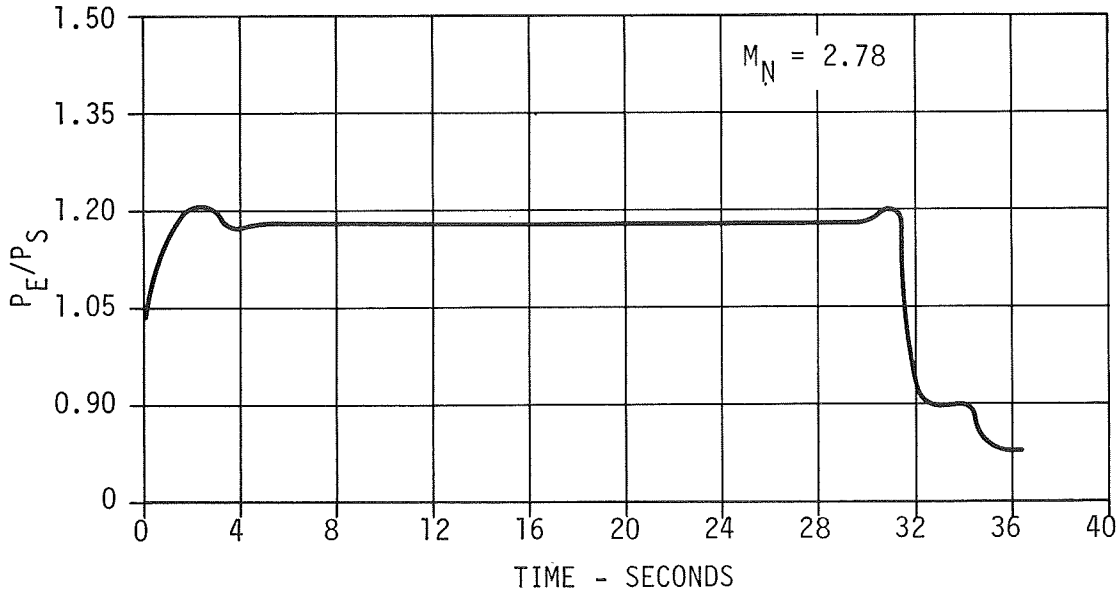

Figure 2-18. VARIATION OF P_E/P_S WITH TIME FOR 90° STEP MODEL (WITH OUTERWALL EXTENSION)

Section III

FLUCTUATING PRESSURE, VIBRATION AND ACOUSTIC CHARACTERISTICS OF THE SPECIAL TEST SECTION

3.1 OBJECTIVES

An extensive instrumentation set-up was made for this test phase because previous experience with the original special test section had indicated that the pressure fluctuations measured on boundary-layer and 90-degree-step models by use of conventionally mounted pressure transducers were severely modified by extraneous effects. An attempt to measure the pressure fluctuations in the undisturbed flow, to establish their role in the extraneous contributions, failed because of a malfunction of one of the transducers on the probe specially designed for this purpose. However, the objectives of the successful portion of the tests performed were as follows:

- To establish levels of pressure fluctuations in the various flow regions of the test section, and to determine how measurement of fluctuating pressures is affected by the size of the pressure transducer and the method in which the transducers are mounted.
- To establish the levels of random vibrations, and to determine what effect these random vibrations have on measurement of fluctuating pressures in these regions.
- Establish the correlation between the fluctuating pressures observed in the tunnel and the acoustic field created in the test cell.

The tunnel run schedule for these tests is given in Table 2-3.

3.2 INSTRUMENTATION

The basic instrumentation used for obtaining the dynamic data consisted of transducers and accelerometers for measuring fluctuating pressures and vibrations or acoustic pressures and accelerations, respectively. The characteristics of this instrumentation are given in Table 3-1 and a wiring diagram is presented in Figure 3-1. Transducer locations may be divided into regions of the test section as described in the following subsection.

Table 3-1. CHARACTERISTICS OF VARIOUS TRANSDUCERS AND ACCELEROMETERS USED FOR DYNAMIC CALIBRATION

IDENTIFICATION	SIZE	SENSITIVITY RANGE	SENSITIVITY AREA	VIBRATION CHARACTERISTICS	TEMPERATURE CHARACTERISTICS
A. Pressure Transducers					
601L KISTLER	.25 In. dia.	0.1 to 300 psi @ .5 percent linearity	.0493 $In.^2$	Resonates at 130,000 cps, max shock=15,000 g's	-450 to 500°F @ 0.01 percent/°F
BYTREX HFD-2	.125 In. dia.	0 to 2 psi @ .5 percent linearity	.0123 $In.^2$	Resonates at 60,000 cps	30 to 180°F @ .03 percent/°F
B. Accelerometers					
ENDEVCO 2220C	0.375 In. dia.	0 to 5000 g, Sensitivity increases 1 percent/ 500 g		± 5% from 2Hz to 10,000 H_z	± 10% °C(-54 to 177) °F(-65 - 350)
KISTLER 808	0.5 In. Hex, 0.9 In. long	0 to 10,000 g		Mean DC to 7,000Hz to 5%	-320 to + 500 °F
C. Condenser Microphone					
B&K TYPE 4135	0.25 dia	760 mm @ 250Hz @ 200V	.0493 $In.^2$	Very sensitive to vibration, 1g 88db must be properly mounted	+ 0.5 db from -40 to + 200°C -40 to + 392°F

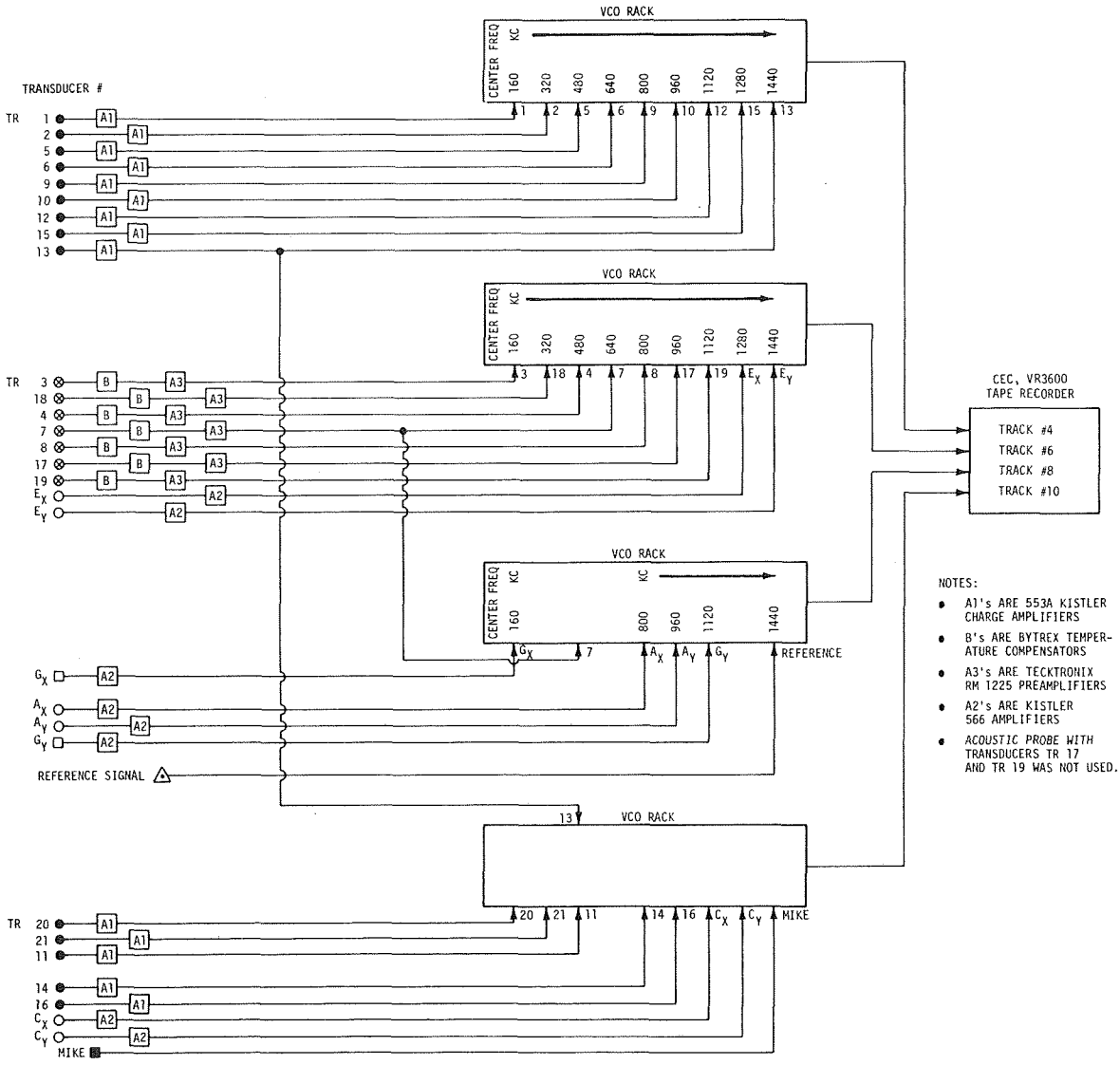

Figure 3-1. DYNAMIC DATA RECORDING SCHEME

3.2.1 Upstream Transducers

In the upstream region (the settling chamber, the supporting struts, and the subsonic portion of the plug) five pressure transducers no. 1, 2, 3, 4, and 18 were located as shown in Figure 3-2. As depicted in this figure, transducers no. 1 and 2 were Kistler 601L and no. 3, 4, and 18 were Bytrex HFD-2. The anticipated RMS levels of the random vibration in this region were less than 1g because of small flow velocities and rigid structural connections; therefore, no accelerometers were located in this region and all the transducers were mounted by conventional metal-to-metal contact. This transducer-mounting scheme is referred to as "hard mounting" in this report.

Transducer no. 1 and 3 measure the plenum chamber-pressure fluctuations and transducer no. 2 detects changes in the pressure fluctuation levels caused by the flow through the abrupt cross-section reduction at the interface of the test section and settling chamber. A direct comparison between data from transducer no. 1 and 3 should provide a qualitative estimate of the effect of transducer size in low velocity flows.

Transducer no. 4 and 18 were placed to detect the effect of screens on the ambient-pressure fluctuations. Additionally, transducer no. 4 was located directly downstream of the support strut, thereby indicating the effectiveness of screens for dispersing the strut wake.

3.2.2 Plug Extension Transducers

The flow field of primary interest was close to the downstream end of the plug, because step, protuberance, and multiple jet models will be attached there during future tests. Consequently, the plug extension was equipped with eight pressure transducers and two accelerometers, located as shown in Figure 3-3.

Six of these pressure transducers were Kistler 601L and the remaining two were Bytrex HFD-2. Two Kistler transducers were hard-mounted, (no. 12 and 15), two were soft-mounted (no. 5 and 6) by using specially prepared rubber grommets, and the remaining two (no. 20 and 21) were mounted inside the plug

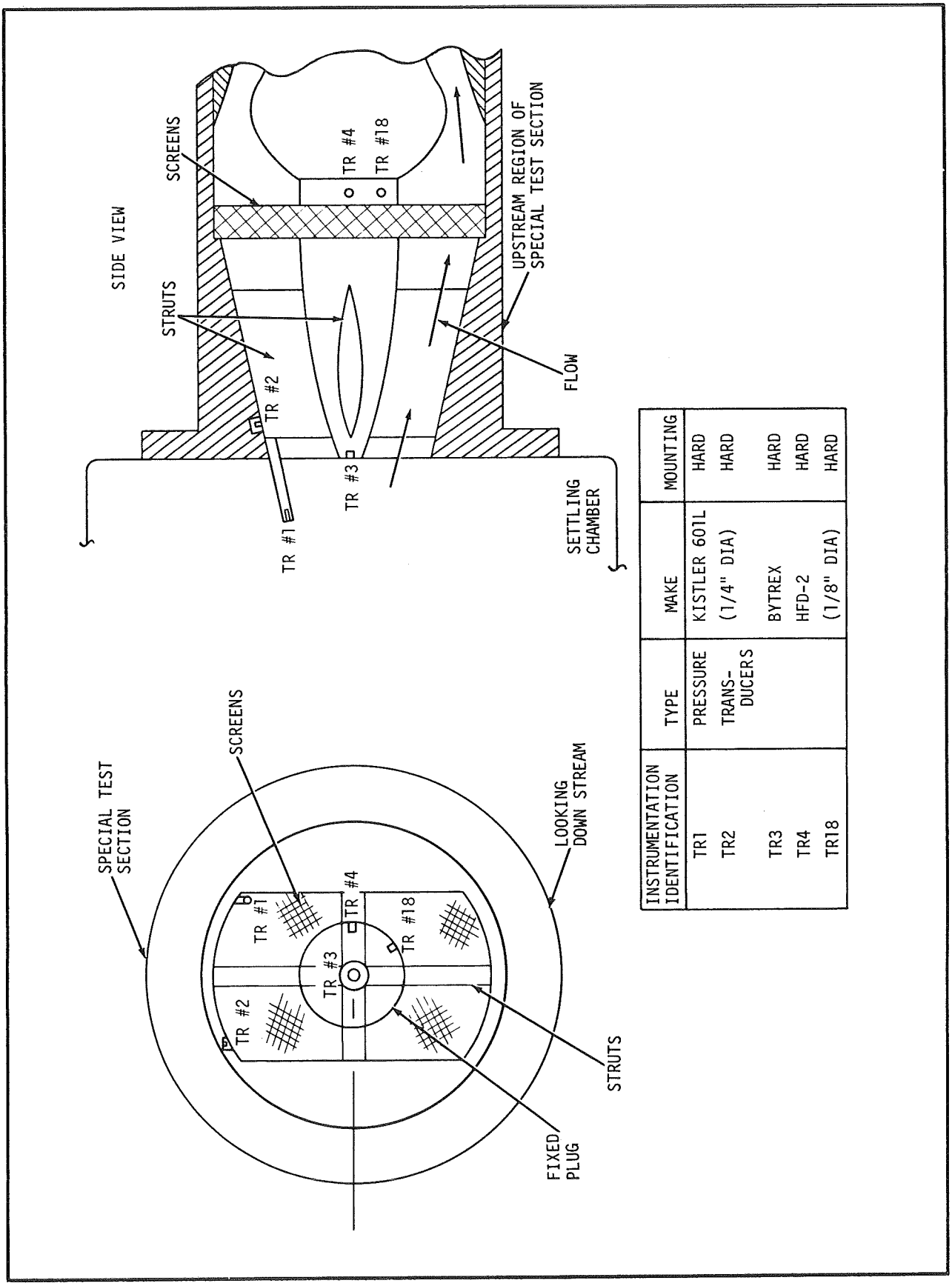

INSTRUMENTATION IDENTIFICATION	TYPE	MAKE	MOUNTING
TR1	PRESSURE TRANS-DUCERS	KISTLER 601L (1/4" DIA)	HARD
TR2			HARD
TR3		BYTREX HFD-2 (1/8" DIA)	HARD
TR4			HARD
TR18			HARD

Figure 3-2. LOCATIONS OF UPSTREAM PRESSURE TRANSDUCERS

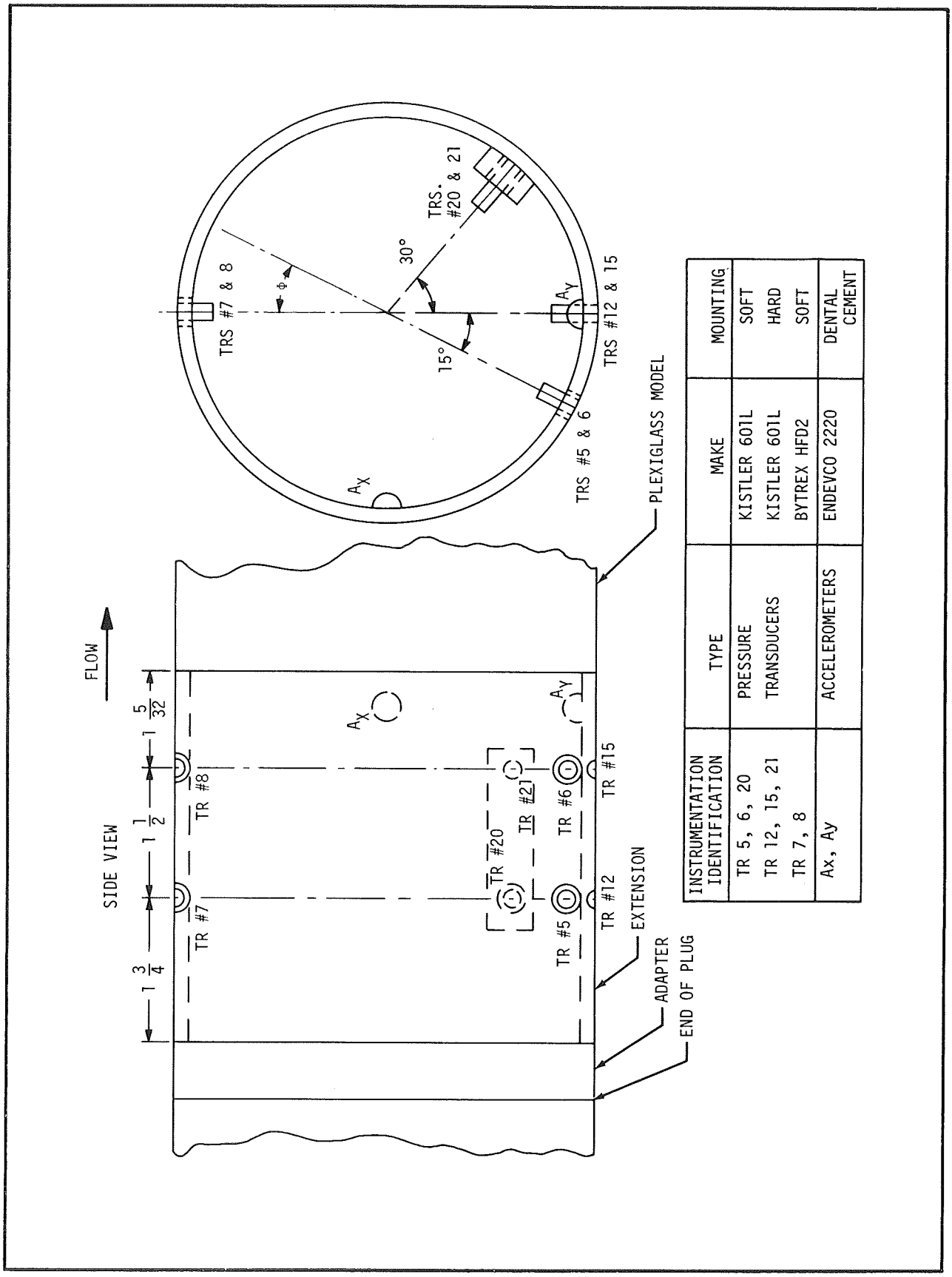

INSTRUMENTATION IDENTIFICATION	TYPE	MAKE	MOUNTING
TR 5, 6, 20	PRESSURE TRANSDUCERS	KISTLER 601L	SOFT
TR 12, 15, 21		KISTLER 601L	HARD
TR 7, 8		BYTREX HFD2	SOFT
Ax, Ay	ACCELEROMETERS	ENDEVCO 2220	DENTAL CEMENT

Figure 3-3. TRANSDUCER AND ACCELEROMETER LOCATIONS ON INSTRUMENTED EXTENSION

extension on a bar. The upstream (no. 20) Kistler transducer was soft-mounted inside the plug extension while the downstream transducer (no. 21) was hard-mounted. Both the Bytrex transducers (no. 7 and 8) were soft-mounted. The two Endevco 2220 accelerometers (Ax and Ay) were oriented to measure vertical and horizontal components of accelerations due to structural vibrations.

3.2.3 Transducers on the Outerwall and Its Extension

Two Endevco 2220 Accelerometers (Cx and Cy) were located approximately 3 inches upstream of the exit plane of the outerwall in a manner to allow measurement of vertical and horizontal accelerations of the outerwall due to its random vibrations.

Two Kistler 601L pressure transducers (no. 9 and 10) were located on the 6-inch Plexiglas extension approximately 5 inches upstream of its exit plane.

The axial and angular locations of these transducers are shown in Figure 3-4.

3.2.4 Window Section Transducers

Two Endevco 2220 accelerometers (Ex and Ey) were located inside the window section to ascertain vertical and horizontal acceleration of the window section.

Also, four Kistler 601L transducers were hard-mounted on a bar attached to a loop of heavy tygon tubing to isolate the transducers from random structural vibrations of the window section (Figure A-9). The axial and angular positions of these transducers, along with their method of mounting, are shown in Figure 3-5.

3.2.5 Guide Rail Accelerometers

Two Kistler accelerometers (Gx and Gy) were mounted on the wind tunnel guide rails to determine the level of structural vibrations transmitted to the ground (Figure 2-2).

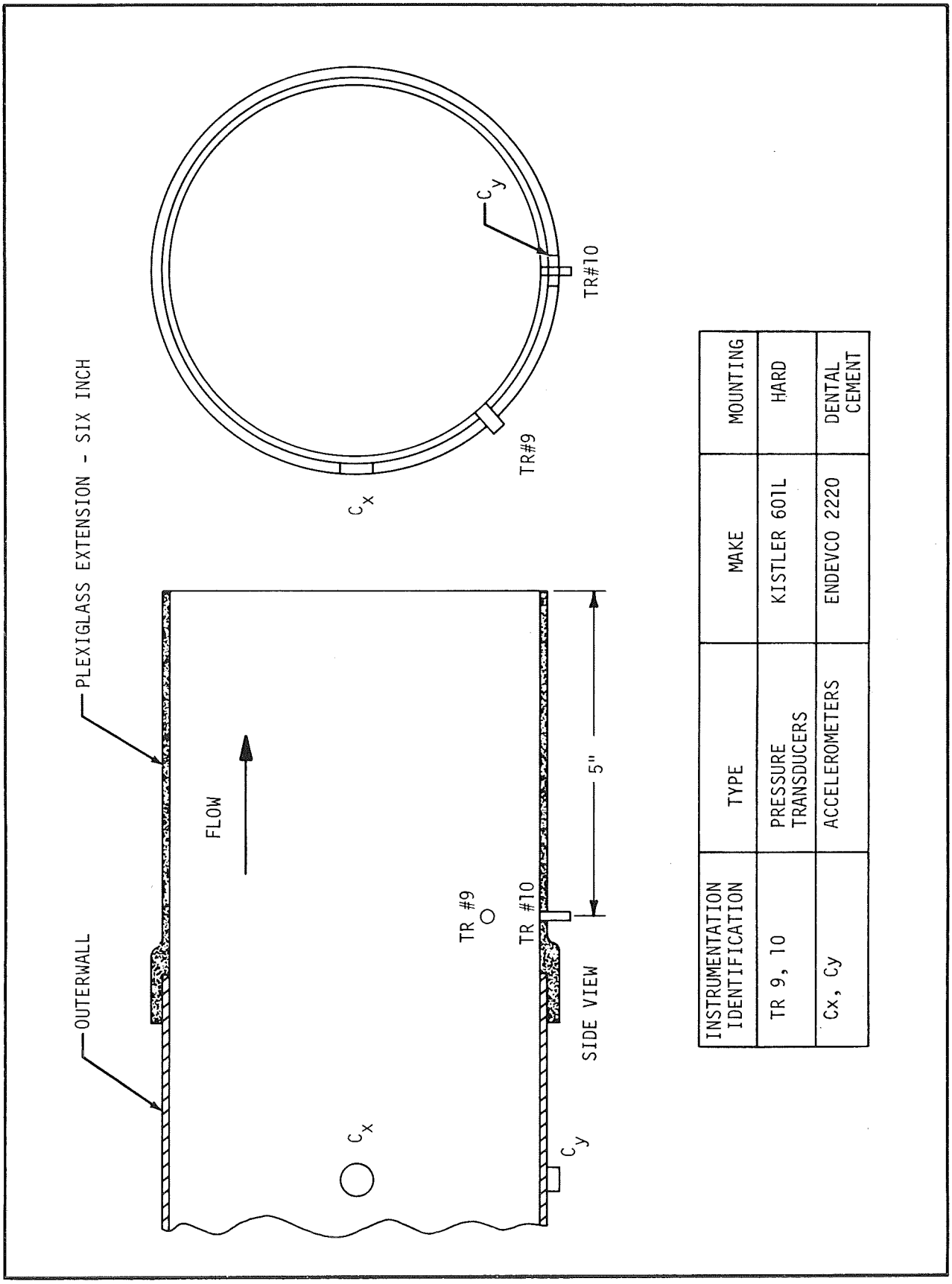

INSTRUMENTATION IDENTIFICATION	TYPE	MAKE	MOUNTING
TR 9, 10	PRESSURE TRANSDUCERS	KISTLER 601L	HARD
Cx, Cy	ACCELEROMETERS	ENDEVCO 2220	DENTAL CEMENT

Figure 3-4. OUTERWALL ACCELEROMETERS AND OUTERWALL EXTENSION PRESSURE TRANSDUCERS

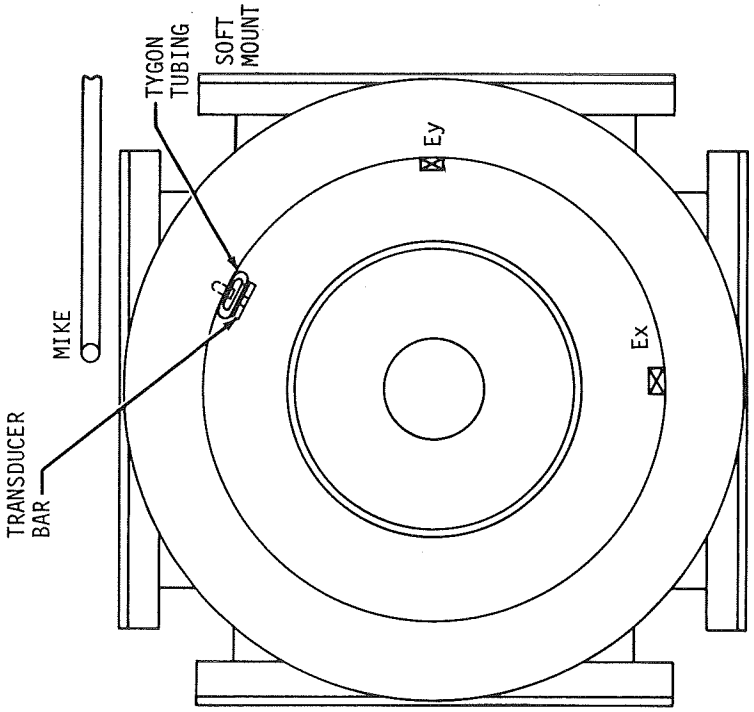

INSTRUMENTATION IDENTIFICATION	TYPE	MAKE	MOUNTING
TR 11, 13, 14, 15	PRESSURE TRANSDUCERS	KISTLER 601L	SOFT MOUNTED BAR
Ex, Ey	ACCELEROMETERS	ENDEVCO 2220	DENTAL CEMENT

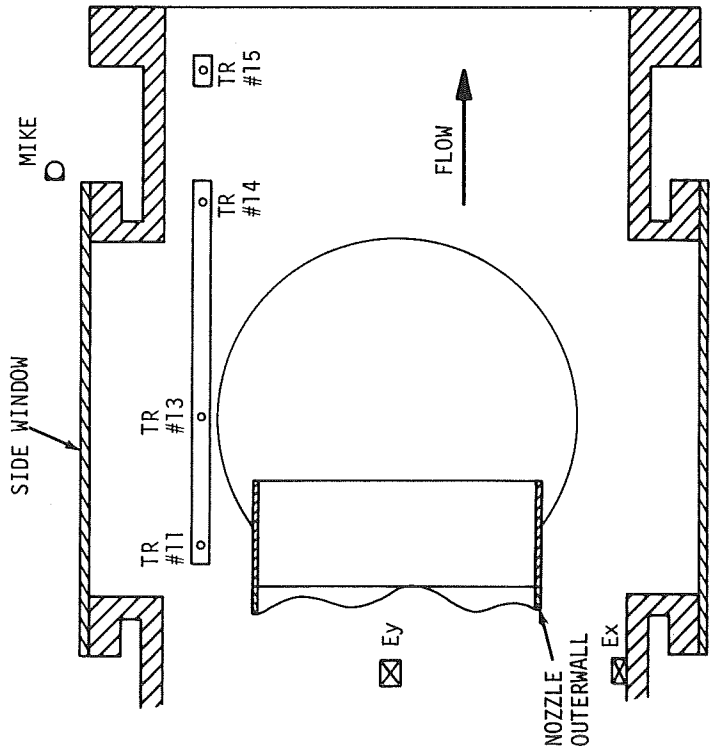

NOTE: MODEL REMOVED

Figure 3-5. LOCATION OF TEST CHAMBER TRANSDUCERS AND ACCELEROMETERS

3.2.6 Test Cell Acoustic Field

The test cell acoustic field was measured by a microphone placed approximately along a line 45 degrees to the axis of the tunnel, 6 feet downstream from the centerline of the windows and 5 feet above the floor level (Figure A-4).

3.2.7 Data Recording

The dynamic data were recorded using the scheme shown in Figure 3-1. Gain settings used for various transducers are shown in Table 3-2.

The length of the cables connecting the 1/4-inch-diameter Kistler transducers and the corresponding charge amplifiers was less than 6 feet in order to keep the cable noise to an acceptable level. This was achieved by locating the amplifiers for the upstream transducers and plug extension transducers inside the plug and by mounting the amplifiers of the outerwall extension and window section transducers inside the window frame (Figure A-8). Additional precaution was taken by mounting all the amplifiers on foam rubber pads to avoid any noise due to cable rubbing and twisting.

The output levels (RMS, as well as peak-to-peak) from each pressure transducer and accelerometer were measured during the static calibration runs at which time no dynamic data was recorded. These measurements were used as a guide to establish the optimum settings of various amplifiers that were accessible for gain settings (i.e., excluding those inside the plug). It was possible to ascertain that the signals were not too large to be clipped or too small to be buried in the noise while they were being recorded on the tape recorder.

3.3 ANALYSIS OF DYNAMIC DATA

3.3.1 Upstream Pressure Fluctuations

Figure 3-6 shows the RMS levels of pressure fluctuations for various transducers in the upstream subsonic portion of the test section for runs corresponding to a nominal pressure of 30 psia in the settling chamber. On the acoustic scale these values correspond to 149 through 155 db (Reference 0.0002 dynes/cm^2), which is a fairly high level. Thus, it appears that the flow field

Table 3-2. TRANSDUCER GAINS AND FULL SCALE VCO SETTINGS USED IN THE TESTS

TAPE TRACK NO.	INSTRUMENTATION NO.	VCO FULL SCALE	INSTRUMENTATION GAIN
4	TR 1, 2, 5, 6, 12, 15	267 MV-PC (189 MV RMS)	1.22 psia-RMS / volts-RMS
10	TR 20, 21, 11	267 MV-PC (189 MV RMS)	1.22 psia-RMS / volts-RMS
4	TR 9, 10, 13	1.13 Vols-PC (800 MV RMS)	0.29 psia-RMS / volts-RMS
6	TR 3, 18, 4, 7, 8	1.13 Vols-PC (800 MV RMS)	0.29 psia-RMS / volts-RMS
10	TR 13, 14, 16	1.13 Vols-PC (800 MV RMS)	0.29 psia-RMS / volts-RMS
8	TR 7	2 volts DC	0.29 g's-RMS / volts-RMS
6	Ex,Ey	-	17.1 g's-RMS / volts-RMS
8	Gx	-	40 g's-RMS / volts-RMS
8	Gy	-	40.03 g's-RMS / volts-RMS
8	Ax	-	7.175 g's-RMS / volts-RMS
8	Ay	-	7.2 g's-RMS / volts-RMS
10	Cx	-	68 g's-RMS / volts-RMS
10	Cy	-	71 g's-RMS / volts-RMS
10	Mike	-	1.22 psia-RMS / volts-RMS

NOTE: Calibration signal is 189 mV RMS (267 mV 0-peak) at 1 KHz. (Before applying the gains the observed levels should be scaled according to the level of calibration used.)

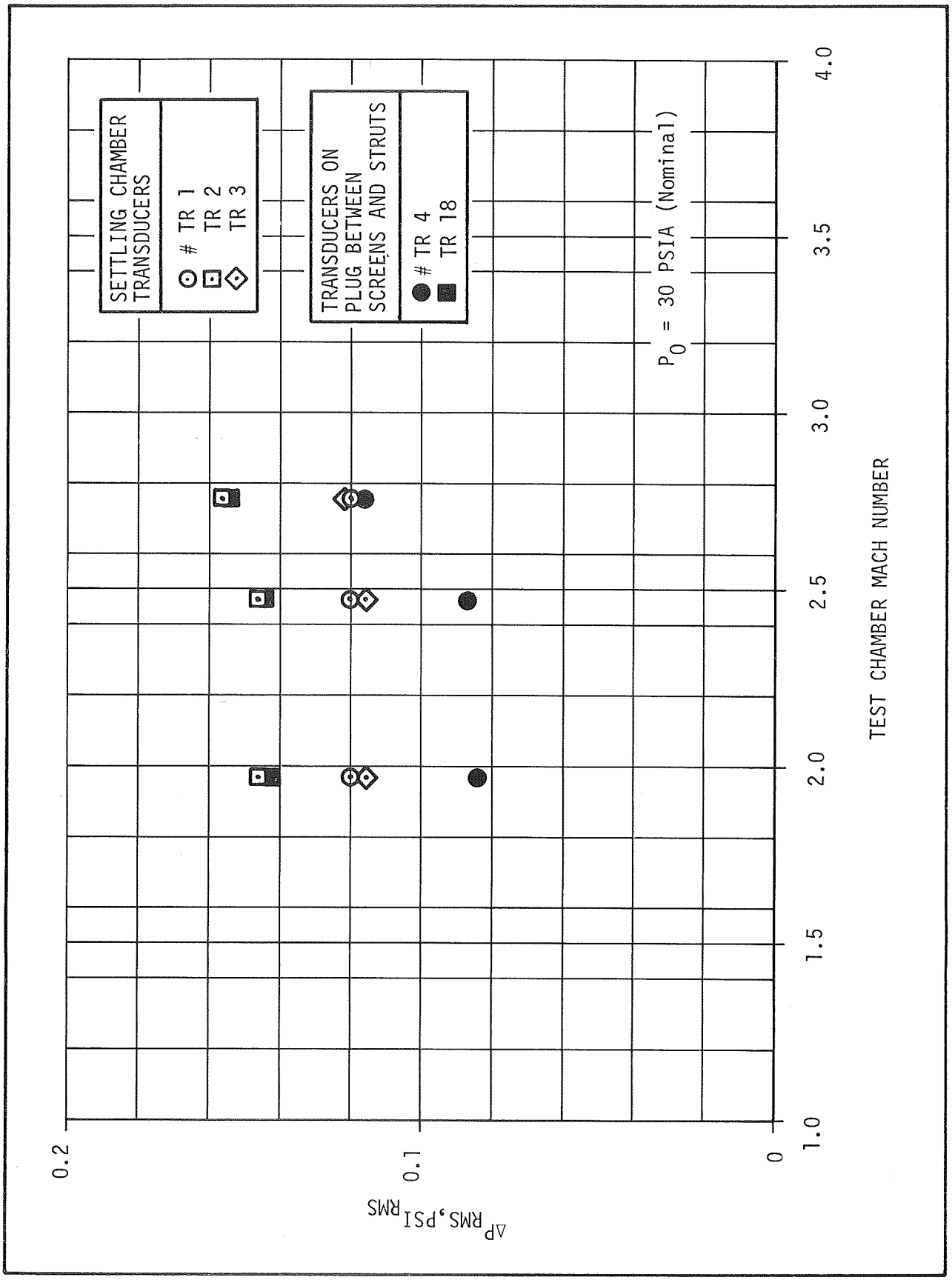

Figure 3-6. RMS INTENSITY OF UPSTREAM (SUBSONIC REGIME) PRESSURE FLUCTUATIONS

has a high acoustic level that may be originating from the various flow turns and valves.

The size of a particular transducer significantly influences fluctuating measurements when the eddy scale is of a comparable magnitude; consequently, indications are that eddies in this region are quite large because two different pressure transducers sizes (1/4-inch and 1/8-inch diameter) produced essentially the same results.

As the flow is accelerated in the entrance of the test section, the level of pressure fluctuations increases by about 5 db (at 30 psia nominal pressure). The effect of the strut wake and the screens combined reduce the level by approximately 1 db; however, the screen itself reduces the pressure fluctuations by a negligible amount. The strut probably provides an obstruction to the acoustic rays, whereas the screen allows fluctuations to penetrate without significant damping. This result suggests that the plug itself can be reflecting the ambient acoustic waves of frequencies above approximately 500 Hz (Velocity of sound $\sim$ 1000 ft/sec, plug maximum diameter $\sim$ 2 ft). It may also be observed that the pressure levels depend only on the upstream conditions in this region because disturbances cannot be transmitted upstream through the sonic throat.

A typical autocorrelation curve for the upstream pressure fluctuations is shown in Figure 3-7. The range of frequencies for these data was 0 to 20 KHz.

3.3.2 Plug Extension Pressure Fluctuations and Accelerations

As shown in Figure 3-3, the plug extension was heavily instrumented. This extension was also rotated through various azimuthal positions, as indicated in Table 2-3. Figure 3-8 shows ΔC_pRMS, the RMS pressure fluctuations which are nondimensionalized with respect to q, the dynamic pressure.

The Bytrex transducers (no. TR7 and 8) give ΔC_pRMS of 0.08, whereas the Kistler transducers (no. TR5, 6, 12, 15, 20, and 21) give ΔC_pRMS in the range of

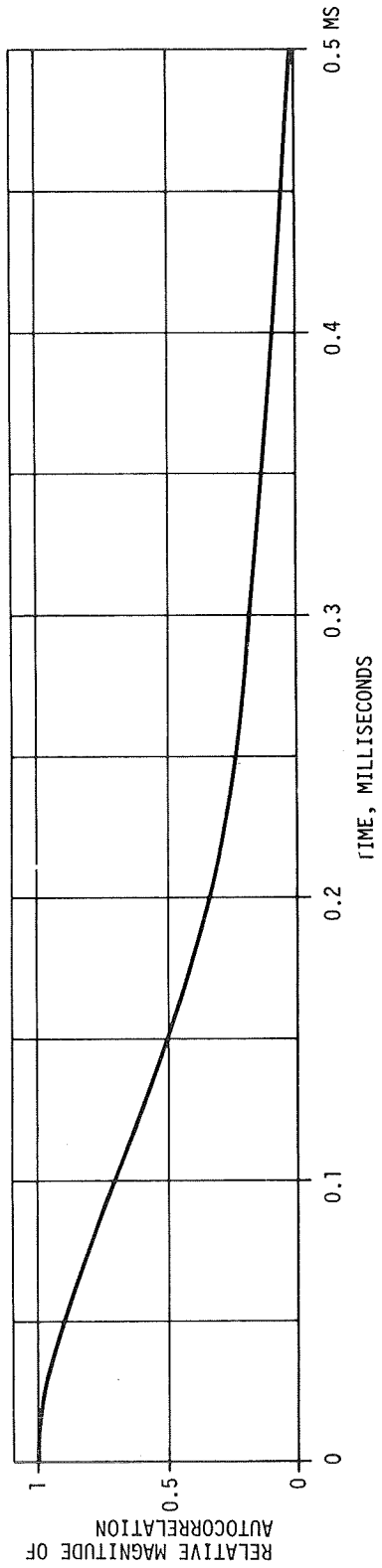

Figure 3-7. TYPICAL AUTOCORRELATION OF UPSTREAM (SUBSONIC REGIME) TRANSDUCER

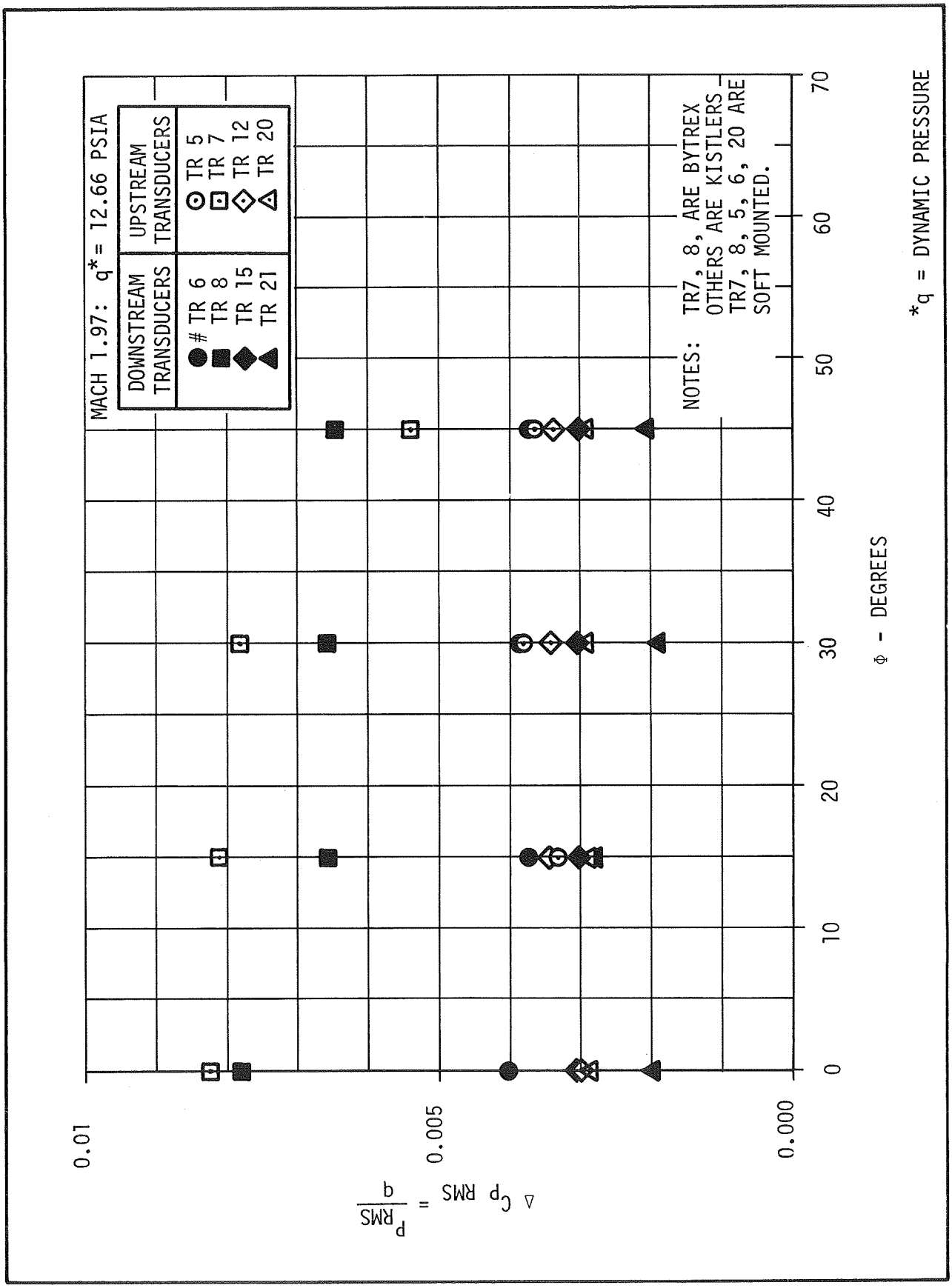

Figure 3-8. VARIATION OF ACOUSTIC FIELD WITH ANGULAR POSITION

0.02 to 0.04. Such large differences cannot be accounted for by the size difference of the transducers. Additionally, the transducers (no. 20 and 21) that are not exposed to the flow measure approximately the same ΔC_PRMS as those exposed to the flow. However, these pressure fluctuations have a typical frequency of 333 Hz (Figure 3-9). This paradox is not caused by severe random structural vibrations of the plug because the accelerometers Ax and Ay indicate acceleration levels to be in the range of 2g's RMS (Table 3-3), which would account for only 10 percent of the ΔC_PRMS. These results indicate some extraneous phenomena such as vibration of the bar on which transducers no. 20 and 21 are mounted or severe breathing in the plug cavity. It is therefore necessary to examine other techniques for measurement of pressure fluctuations on the plug extension. The actual values of the ΔPRMS (RMS pressure fluctuations) are given in Table 3-4.

A typical autocorrelation (Figure 3-10) of the plug extension transducers that are exposed to the flow indicates a broadband spectral characteristic for the pressure fluctuations, and a typical cross-correlation (Figure 3-11 (a), (b), (c), (d), (e), (f), (g), (h), and (i)) of two transducers separated along the axis (such as no. 5 and 6 or 12 and 15) gives a convection speed $U_c \simeq 0.8\ V_\infty$. It is observed that these measurements indicate the presence of an extraneous correlatable signal which arises typically in any one or more of the three pairs of transducers, at a given Mach number.

3.3.3 Pressure Fluctuations and Vibrations of the Outerwall Extension and Window Cavity

Figure 3-12 gives the ΔC_PRMS for transducer numbers 9 and 10 (located on outerwall extension - Figure 3-4), and 11, 13, 14, and 15 (located in the window section - Figure 3-5). At lower Mach numbers the ΔC_PRMS increases for all transducers because the shock structure is much stronger and its oscillations are the major contributing factor to the ΔC_PRMS at the locations of the transducers mentioned above. The ΔC_PRMS of transducers no. 13 and 14 are in the range of 0.0067 to 0.0015, whereas, the transducers on the outerwall extension show much higher fluctuation levels. This indicates that the pressure fluctuations measured by the outerwall transducers are not only a result of pressure

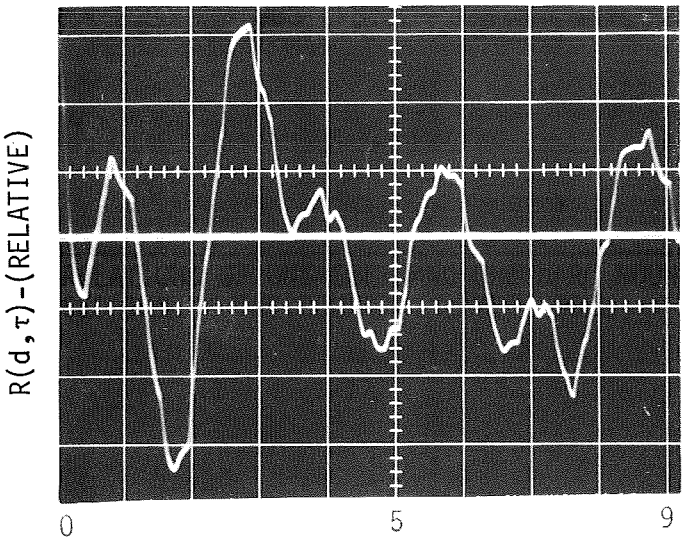

M = 2, f = 333 CPS.

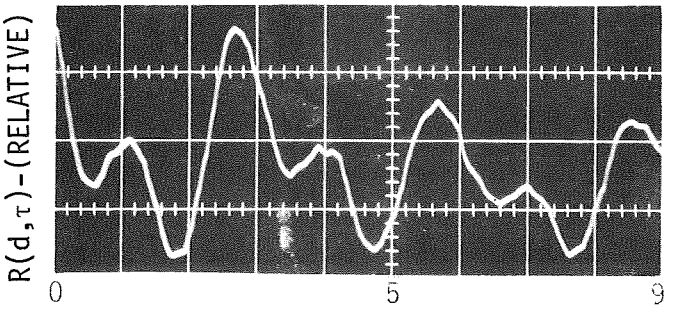

M = 2.8, f = 333 CPS.

Figure 3-9. CORRELATIONS OF ONE SOFT AND ONE HARD MOUNTED TRANSDUCER PLACED INSIDE THE BOUNDARY LAYER MODEL

Table 3-3. ACCELERATIONS OF THE TEST SECTION COMPONENTS

Model Configuration	Outerwall Ext	Ax	Ay	Ex	Ey	Cx	Cy
1	6"	1.27	1.46	0.512	2.65	-	-
1	6"	1.3	3.06	0.684	4.7	14.7	17.2
1	6"	1.02	1.42	0.547	1.366	5.45	5.45
1	6"	1.05	1.39	0.512	1.264	4.7	4.7
2	6"	1.6	1.35	0.51	1.37	5.05	4.98
2	6"	2.4	1.9	0.61	3.24	16.7	21.0
4	6"	1.67	3.32	0.505	3.59	25.9	28.0
4	6"	1.67	3.29	0.505	3.59	26.6	27.6
1	6"	1.67	1.72	0.512	2.74	12.6	15.4
1	6"	1.64	1.53	0.51	2.77	12.6	15.4
1	6"	1.71	1.49	0.512	2.78	13.3	16.1
1	6"	1.71	1.42	0.515	2.82	13.3	15.4
1	none	1.89	1.97	0.512	4.19	-	-
3	6"	1.45	3.28	0.505	4.27	19.6	21.7
2	6"	-	-	0.51	2.39		
5	6"	2.7	2.33	0.515	3.5		

NOTE: Ax, Ay are on plug, Cx, Cy are on the outerwall and
Ex, Ey are on window cavity
All accelerometer data referenced to g

Table 3-4. RMS PRESSURE FLUCTUATIONS OF VARIOUS TRANSDUCERS

Run	101/2	104	105	106	108	115/1	117
Model Config.	1	1	1	2	4	3	1
Outerwall Extension	6"	6"	6"	6"	6"	6"	6"
q. (psia)	12.66	9.21	7.27	7.25	12.97	12.80	12.80
Upstream Transducers	ΔCP RMS for upstream transducers, ($P_{RMS/q}$)						
TR 1	.00948	.0131	.0166	.0163	.00925	.00953	.00945
2	.0115	.0159	.0215	.0211	.0113	.0114	.0114
3	.00916	.0126	.0168	.0168	.00914	.00906	.00906
4	.00664	.00948	.0160	.0160	.00671	.00680	.00679
18	.0112	.0158	.0213	.0213	.00060	.0111	.0113
Plug Extension Transducers	ΔCP RMS for plug extension transducers, ($P_{RMS/q}$)						
TR 5	-	-	-	-	-	-	.00476
6	.00404	.00286	.00304	.00286	.00405	.00367	.00486
12	.00300	.00233	.00253	.00244	.00386	.00372	.00429
15	.00300	.00226	.00244	.00244	.00301	.00295	.00352
20	.00289	.00253	.00454	.00370	.00244	.00315	.00358
21	.00198	.00219	.00286	.00320	.00221	.00209	.00310
7	.00824	.00190	.00253	.00164	.00802	.00812	.00521
8	.00780	.00396	.00304	.00280	.00738	.00725	.00623
Outerwall & Window Cavity Transducers	ΔCP RMS for outerwall & window cavity transducers, ($P_{RMS/q}$)						
TR 9	.0153	.00727	.00605	.00640	.0168	.00498	.0123
10	.00972	.00569	.00685	.00800	.0159	.00544	.0148
11	.0115	.00412	.00380	.00472	-	.0186	-
13	.00367	.00152	.00189	.00232	.00380	.00714	.00477
14	.00664	.00284	.00291	.00400	.00894	.0174	.00883
16	.0125	.00712	.00666	.00901	.0161	.0159	.00149

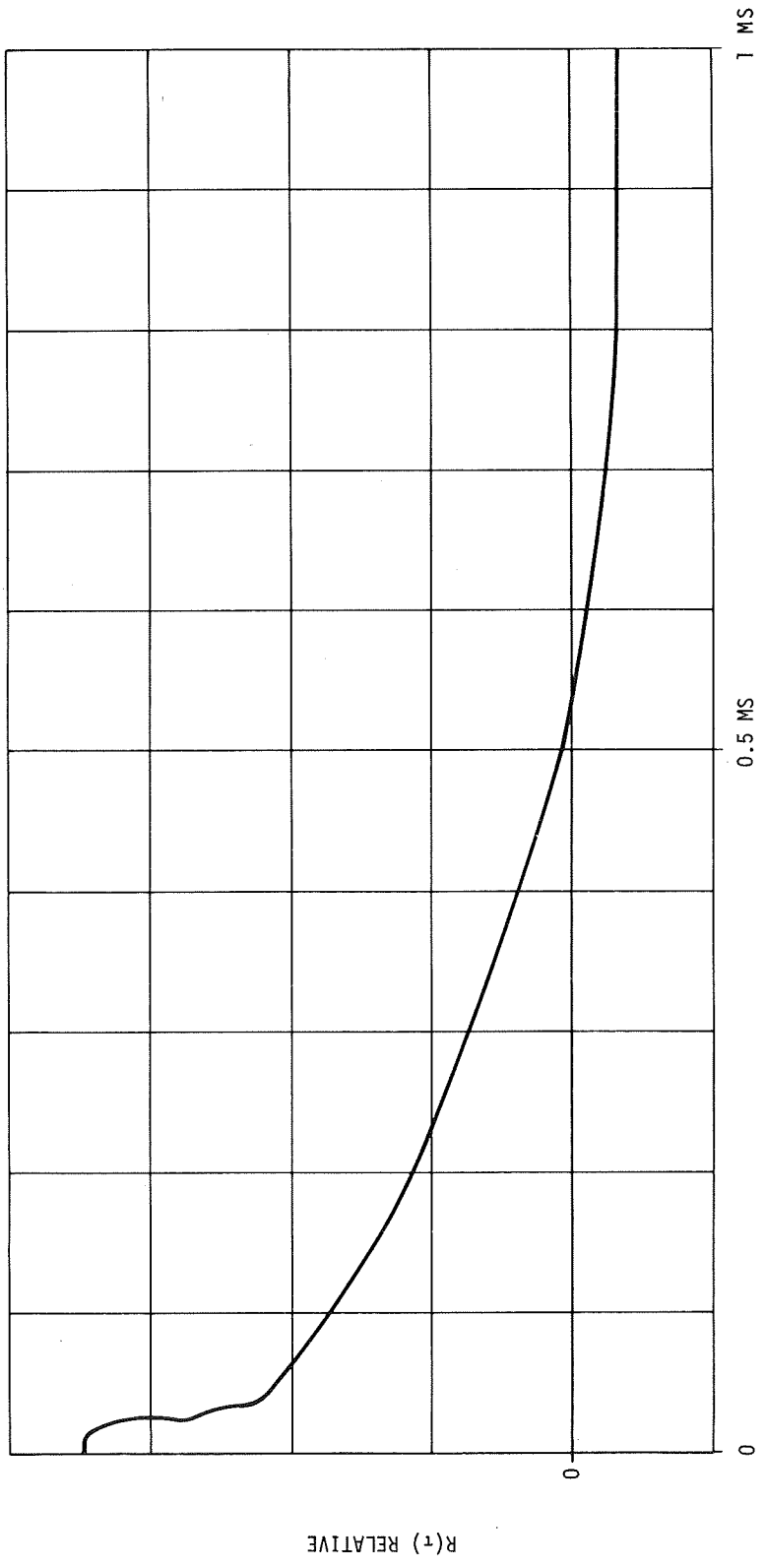

Figure 3-10. TYPICAL AUTOCORRELATION OF PLUG EXTENSION TRANSDUCER EXPOSED TO THE FLOW

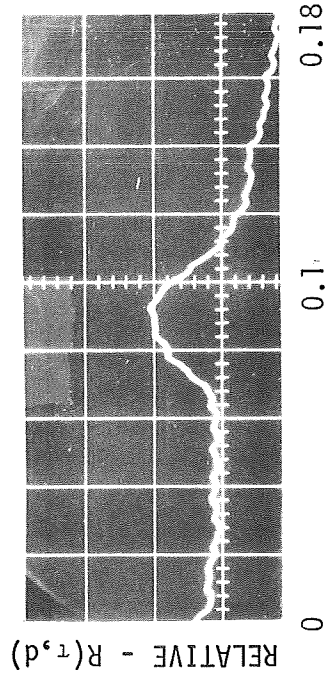

(a) HARD MOUNTED KISTLERS - 601 L

(b) SOFT MOUNTED KISTLERS - 601 L

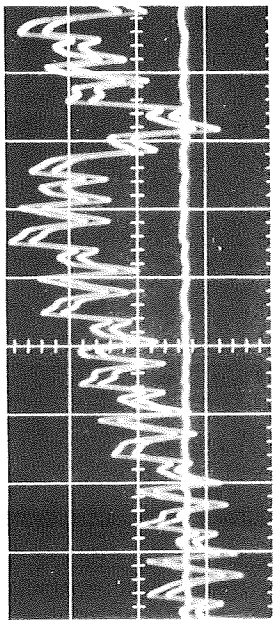

(c) SOFT MOUNTED BYTREX

M = 2, P_o = 35 Psia, CONVECTION SPEED RATIO = $\frac{U_c}{U_\infty}$ = 0.798

Figure 3-11. TYPICAL CORRELATIONS FROM PAIRS OF TRANSDUCERS WHICH WERE MOUNTED DIFFERENTLY ON THE MODEL (BOUNDARY LAYER MODEL - d = AXIAL DISTANCE BETWEEN CORRELATABLE TRANSDUCERS = 1.5 IN.)

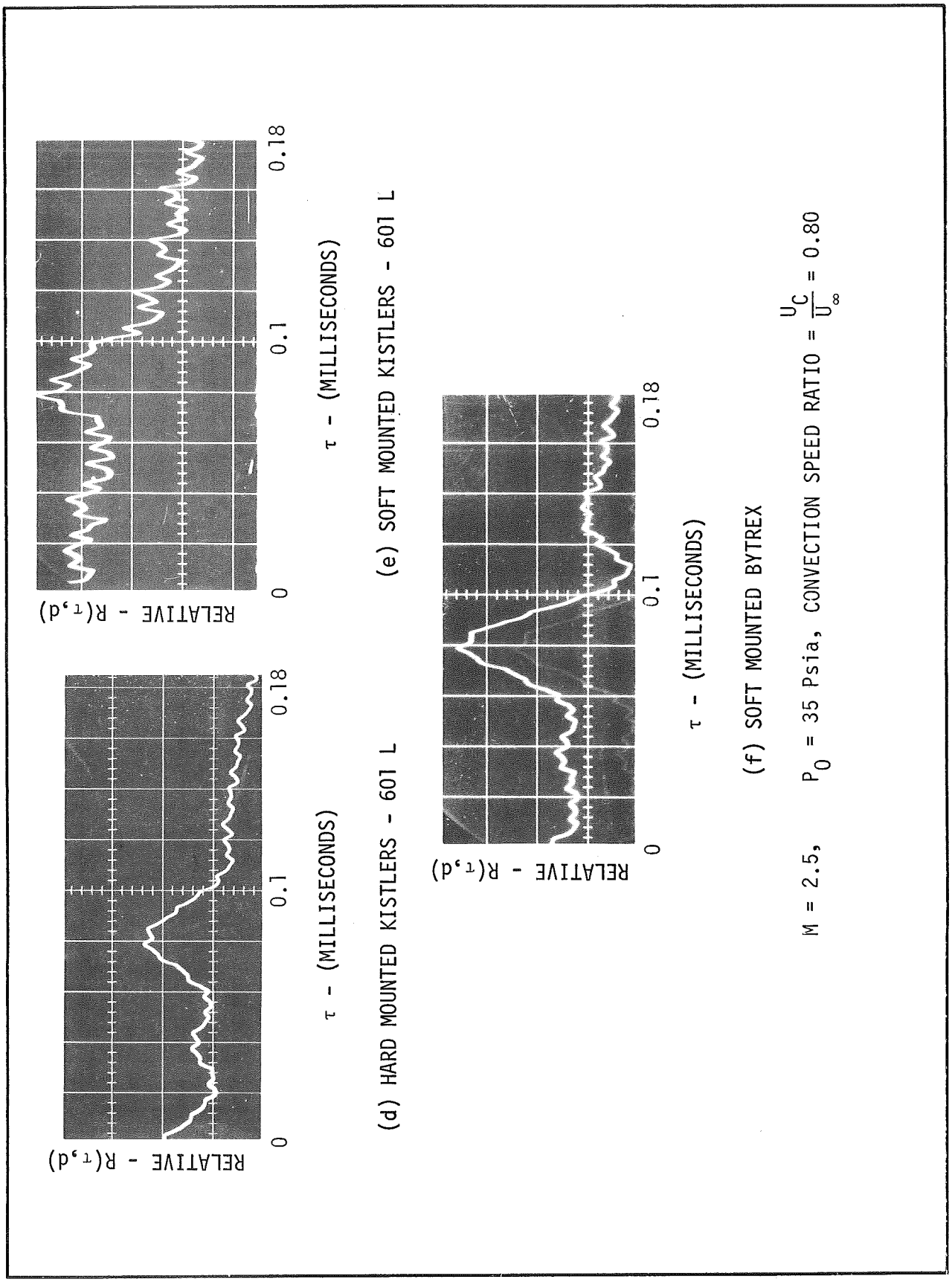

Figure 3-11. TYPICAL CORRELATIONS FROM PAIRS OF TRANSDUCERS WHICH WERE MOUNTED DIFFERENTLY ON THE MODEL (BOUNDARY LAYER MODEL - d = AXIAL DISTANCE BETWEEN CORRELATABLE TRANSDUCERS = 1.5 IN.) (Continued)

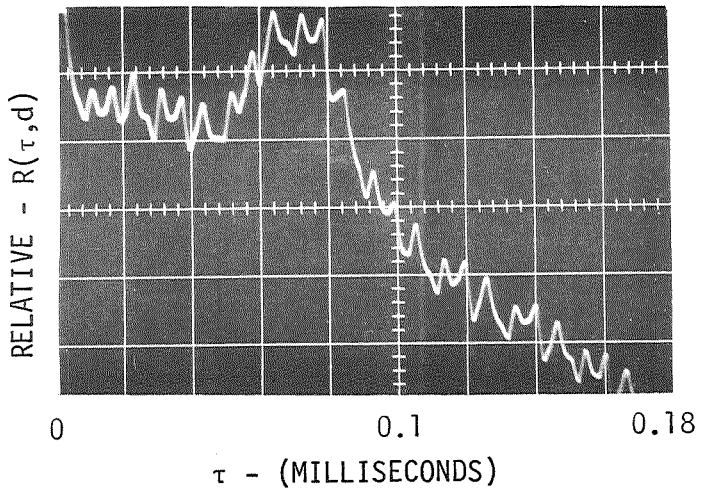

(g) HARD MOUNTED KISTLERS - 601 L

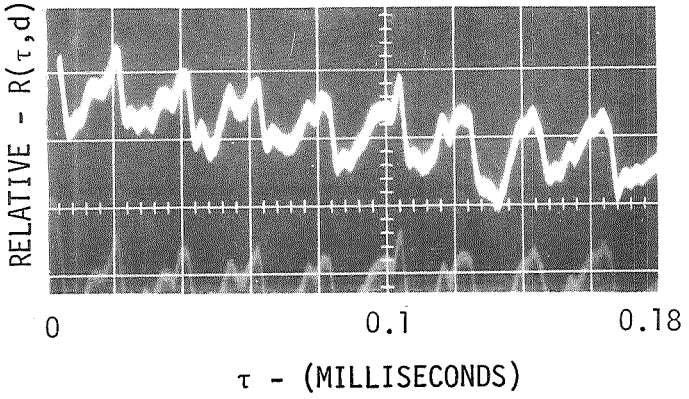

(h) SOFT MOUNTED KISTLERS - 601 L

(UPSTREAM TRANDUCER IS VERY NOISY)

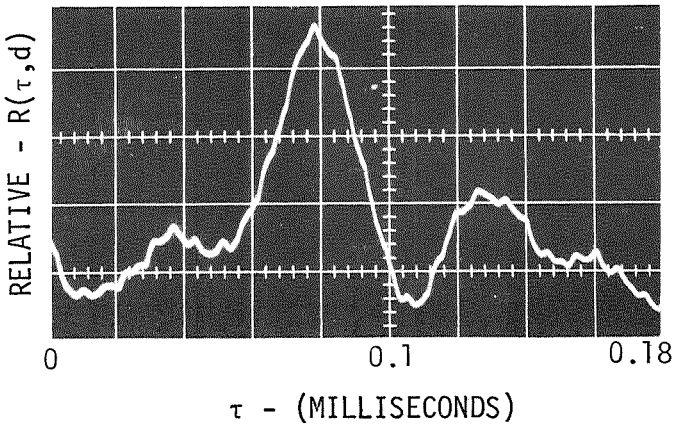

(i) SOFT MOUNTED BYTREX

M = 2.8, P_0 = 3.5, CONVECTION SPEED RATIO = $\frac{U_C}{U_\infty}$ = 0.794

Figure 3-11. TYPICAL CORRELATIONS FROM PAIRS OF TRANSDUCERS WHICH WERE MOUNTED DIFFERENTLY ON THE MODEL (BOUNDARY LAYER MODEL - d = AXIAL DISTANCE BETWEEN CORRELATABLE TRANSDUCERS = 1.5 IN.)(Concluded)

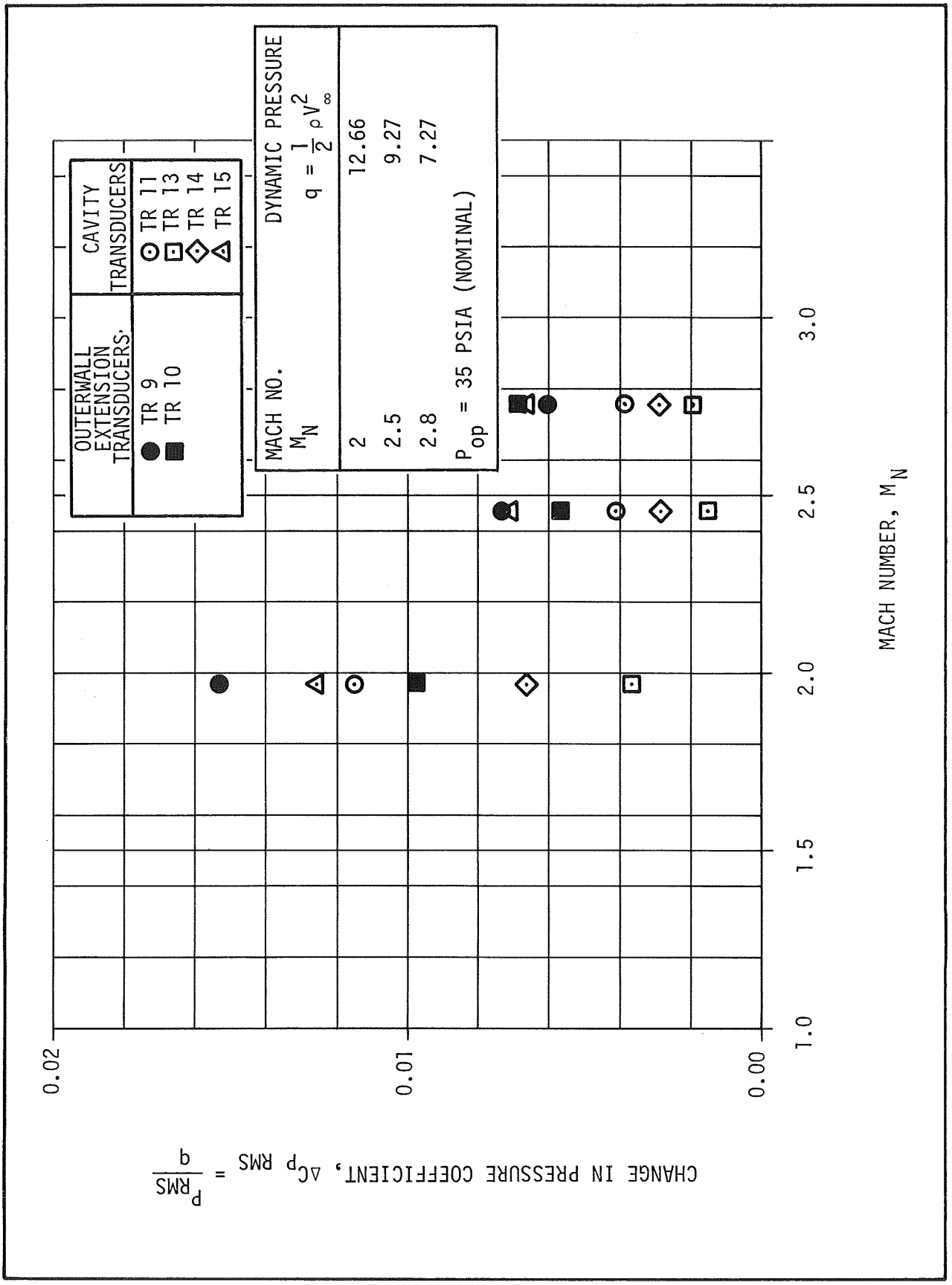

Figure 3-12. TEST SECTION CAVITY AND OUTERWALL EXTENSION TRANSDUCERS

fluctuations associated with the shock at the outerwall exit plane, but are also caused by noise from structural vibrations of the outerwall. Accelerometer data (Table 3-3) corroborate these results. For example, accelerations up to 28 g's at M = 2 are shown. It may, therefore, be necessary to soft-mount the entire outerwall extension to obtain realistic measurements of the pressure fluctuations. The effect of the outerwall extension on the pressure fluctuations in the window cavity may be ascertained by comparing the ΔC_pRMS levels among transducer no. 11, 13, 14, and 16 (Figure 3-13). It is clear that the pressure fluctuation levels are appreciably reduced with the use of the plexiglas extension. This may be attributed to rather efficient flow ducting provided by its use.

The cross-correlation of the window cavity transducers (Figure 3-14) indicate a dominant frequency of fluctuation in the range of 1200 through 1300 Hz for the boundary-layer model and 1330 through 1600 Hz for 90-degree-step model.

3.3.4 Acoustic Environment in the Test Cell

The microphone data were dominated by a 60-cycle per second frequency, and, therefore, did not produce any reliable results.

The only other plausible clue to the acoustic environment in the test cell can be drawn from data of accelerometers Ex, Ey, placed on the tunnel outer walls (Figure 3-5). Ex and Ey measure horizontal and vertical acceleration of the tunnel outerwall (or window section). Typical auto-correlations from these accelerometers show frequencies of 375 and 1600 cps, (Figures 3-15 and 3-16), respectively, for Ex and Ey. Consequently, the acoustic environment will probably lie within that range. Thus, recommendations are that additional study of the test cell environment be conducted in future tests.

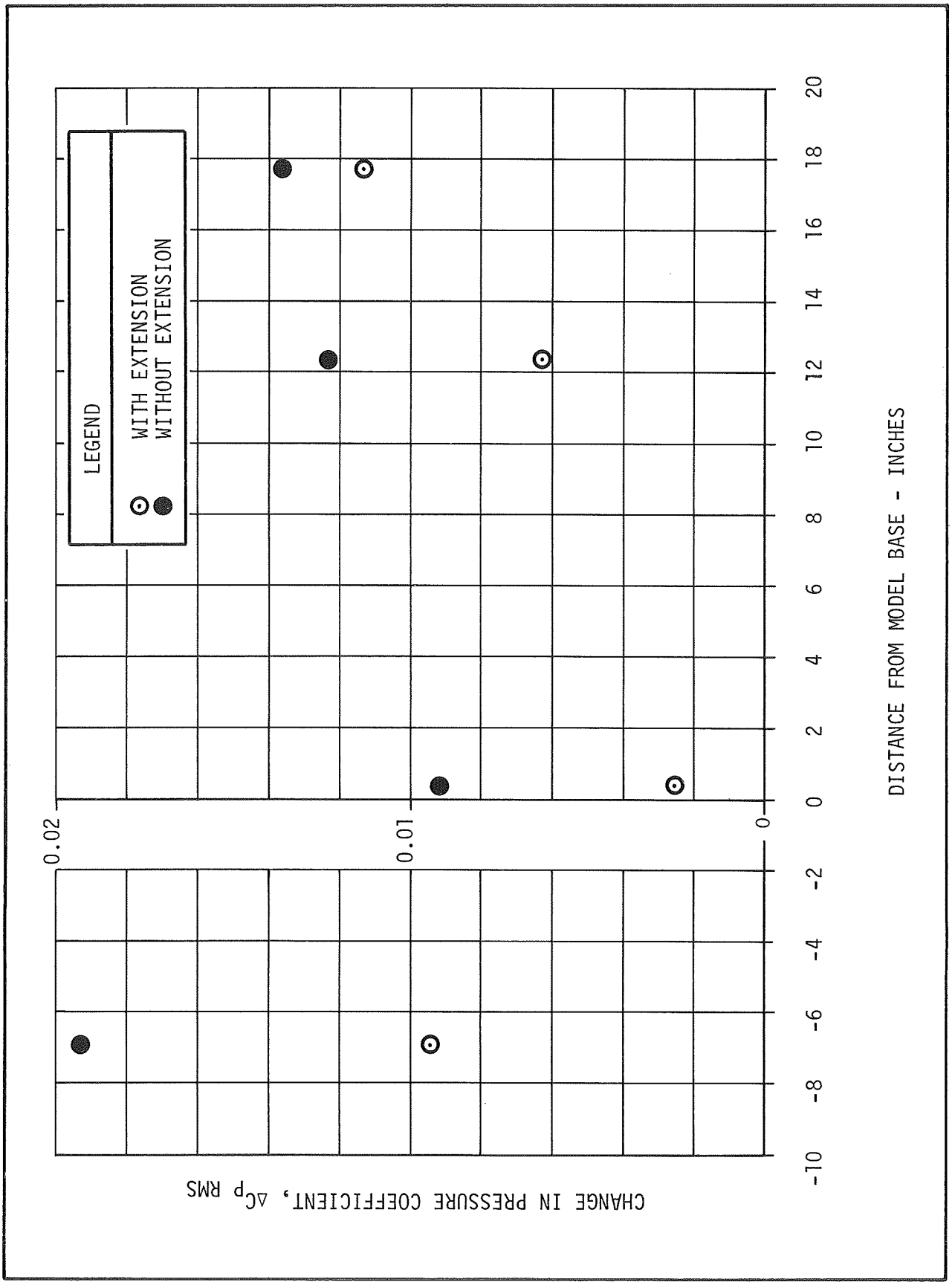

Figure 3-13. EFFECT OF PLASTIC OUTER NOZZLE EXTENSION ON CAVITY PRESSURE FLUCTUATIONS AT MACH 2.0

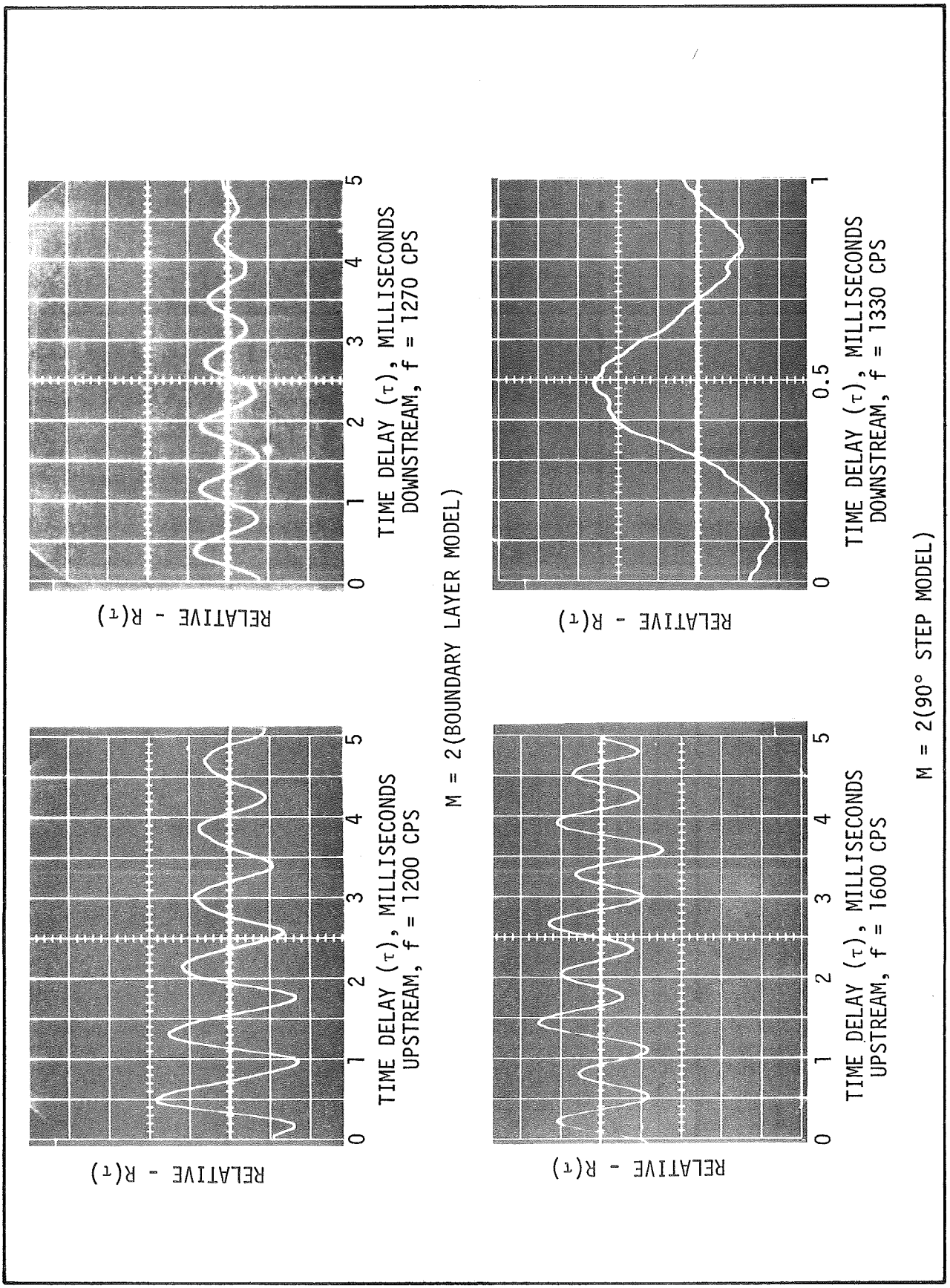

Figure 3-14. TYPICAL CROSS-CORRELATIONS OF WINDOW CAVITY TRANSDUCERS

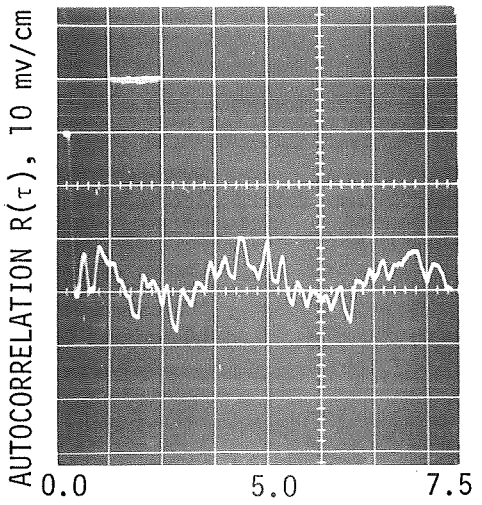

NOTE: FIGURE 3-15.ALSO SHOWS A HIGH FREQUENCY COMPONENT OF ABOUT f ≈ 2500 CPS

Figure 3-15. TYPICAL AUTOCORRELATION OF Ex, THE HORIZONTAL TUNNEL WALL ACCELEROMETER, f ≈ 375 CPS

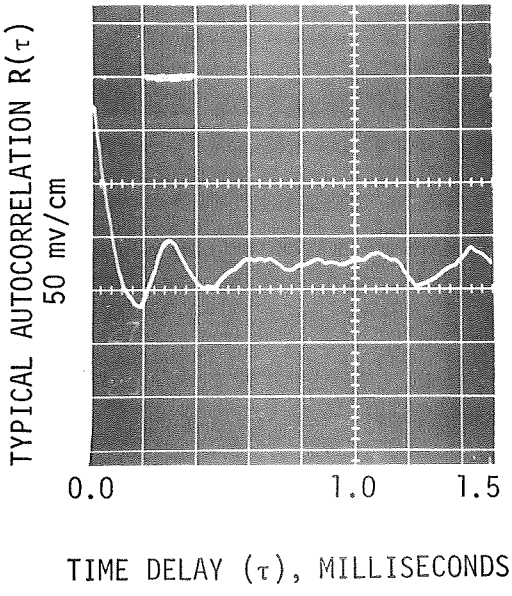

Figure 3-16. TYPICAL AUTOCORRELATION OF Ey, THE VERTICAL TUNNEL WALL ACCELEROMETER, f ≈ 1600 CPS

Section IV
CONCLUSIONS AND RECOMMENDATIONS

The following general conclusions can be drawn from the static and dynamic analysis. These are discussed in the order presented in the report.

4.1 STATIC CALIBRATION CONCLUSIONS

The following conclusions were derived from the analysis of the data presented in Figures 2-7 through 2-16:

- The variation of Mach number with the handcrank counter setting (and hence with the distance between the outerwall-exit plane and the plug downstream end) is linear over the M range of 2.0 through 2.8 for the STS.
- The radial and angular variations of the Mach number for a given outerwall setting are less than .05 and the effect of outerwall extension on this result is negligible. Thus, variation of Mach number is within the range of the instrument system error.
- Dynamic data with stationary mean-flow conditions can be obtained between the sixth and twenty-fourth second of tunnel run time (total 18 seconds), where the zero second corresponds with the time the operator starts the tunnel.

In general, good agreement between experimental results and design calculations were achieved.

4.2 DYNAMIC CALIBRATION CONCLUSIONS

The following conclusions are derived from the analysis of the data presented in Figures 3-6 through 3-16 and Tables 3-1 through 3-3:

- The magnitudes of RMS pressure fluctuations encountered in the upstream subsonic region are too high (148 to 154 db). The screens do not provide any significant noise reduction because of insufficient decay length after the screens. Therefore, it may be advisable to use screens in the inlet section of the settling chamber.
- The magnitudes of RMS pressure fluctuations on the plug are much lower than those of the subsonic regime; however, these measurements have been obscured by too many extraneous effects and the role that the transducer mountings play could not be explicitly determined. The pressure fluctuations inside the cavity are apparently caused by extraneous discrete frequency oscillations of 333 Hz and therefore do not contribute in any manner to the understanding of effects of vibrations on the measurements of pressure fluctuations. The convection speeds of 0.8 V_∞, obtained from cross-correlations of

transducers separated along the flow direction indicate that hard-mounting of transducers is satisfactory for measurements of convection patterns, in separated flows of the types considered here.

- Very high accelerations of the nozzle outerwall (15 to 28 g's) contribute to unacceptable noise levels in the pressure transducer readings.
- The window cavity was subjected to very strong pressure fluctuations, in the frequency range of 1200 to 1600 Hz, probably because of the effect of an oscillating shock structure of the outerwall lip. Window cavity Structural vibration, as a result of these fluctuations, was found to be approximately 3 g's.
- The acoustic field experienced in the test cell is related to vibrations of the window cavity; however, the source could not be explicitly isolated.

Recommendations are that additional precautions be taken during future crossed-beam experiments to insure that fluctuating signals are not merely the result of structural or acoustic vibrations from sources outside the flow field of interest, but do indeed reflect the desired flow phenomenon.

Section V

REFERENCES AND BIBLIOGRAPHY

1. Paranjape, S. V., "Pre-Test Report for the Study of the Characteristics of MSFC's 14-Inch Trisonic Wind Tunnel Special Test Section," Northrop Corporation, Huntsville, Alabama, 10 January 1968.

2. NACA, "Equations, Tables, and Charts for Compressible Flow," NACA Report 1135, Ames Research Staff, 1953.

3. Butler, H. W., "Users Manual, Description of a Digital Computer Program for Nozzle and Plume Analyses by the Method of Characteristics," Lockheed Missiles and Space Company, TM 54/20-108, 11 December 1968.

4. Shapiro, A. H., The Dynamics and Thermodynamics of Compressible Fluid Flow, Vol. I, Ronald Press, New York, 1958.

5. Neighbors, Billy H., "National Aeronautics and Space Administration 14-Inch Tunnel Data Acquisition System," NASA/MSFC R-AERO-AEI Memo for Record, December 13, 1963.

6. Simon, Erwin, "The George C. Marshall Space Flight Centers 14- by 14-Inch Trisonic Wind Tunnel Technical Handbook," NASA TMX-53185, December 22, 1964.

7. Simon, Erwin, "Calibration Tests of the MSFC 14- by 14-Inch Trisonic Wind Tunnel," NASA TMX-63113, August 20, 1964.

8. Johnston, K. D., "Pretest Plans for Pressure Measurements on Step Models in the Special Test Section of the 14-Inch Tunnel," Memorandum R-AERO-AM, 15 February 1967.

9. Crandall, S. H., Random Vibrations, Vol. I & II, MIT Press, Cambridge, Mass., 1963.

10. Seto, W. W., Mechanical Vibrations, Schaum Publishing Co., New York, 1964.

11. Bendat, J. S. and Piersol, A. G., Measurement and Analysis of Random Data, John Wiley, New York, 1966.

12. Funk, B. H., Jr. and Cikanek, H. A., Jr., Optical Probing of Supersonic Aerodynamic Turbulence with Statistical Correlation Phase I: Feasibility, NASA TMX 53850, June 9, 1969.

Appendix

14- BY 14-INCH WIND TUNNEL FACILITY AND PICTORIAL REVIEW OF INSTRUMENTATION MODELS AND TEST SECTION

This appendix presents a pictorial review of the test section instrumentation and models used during these tests. A brief description of the general wind tunnel facility is also included.

A.I WIND TUNNEL FACILITY

The tunnel is an intermittent trisonic blowdown tunnel operated from pressure storage to vacuum or atmospheric exhaust (Figure A-1). The special test section was originally built for the purpose of investigating the base flow phenomena associated with multi-engine boosters. The test section used for this purpose was discussed earlier. Mach numbers range from 1.80 through 2.86 and are obtained by translating the outer nozzle wall.

Air is supplied to a 6000 cubic foot storage tank at approximately -40° F dew point and 500 psi. The compressor is a three-stage reciprocating unit driven by a 1500 hp motor.

The tunnel flow is established and controlled by a servo actuated gate valve. The controlled air flows through the valve diffuser into the stilling chamber and heat exchanger where the air temperature can be regulated from ambient to approximately 180° F. The air then passes through the test section which contains the nozzles and test region.

Downstream of the test section is a hydraulically controlled pitch sector that provides a total angle-of-attack range of 20 degrees ($\pm$ 10 degrees). Sting offsets are also available for obtaining various maximum angles-of-attack up to 25 degrees. This optional equipment was not used in these tests.

The supersonic diffuser has movable floor and ceiling panels that permit more efficient running supersonically. The sector assembly and supersonic diffuser are mounted on guide rails and telescope into the subsonic diffuser to allow easy access to the model and test section.

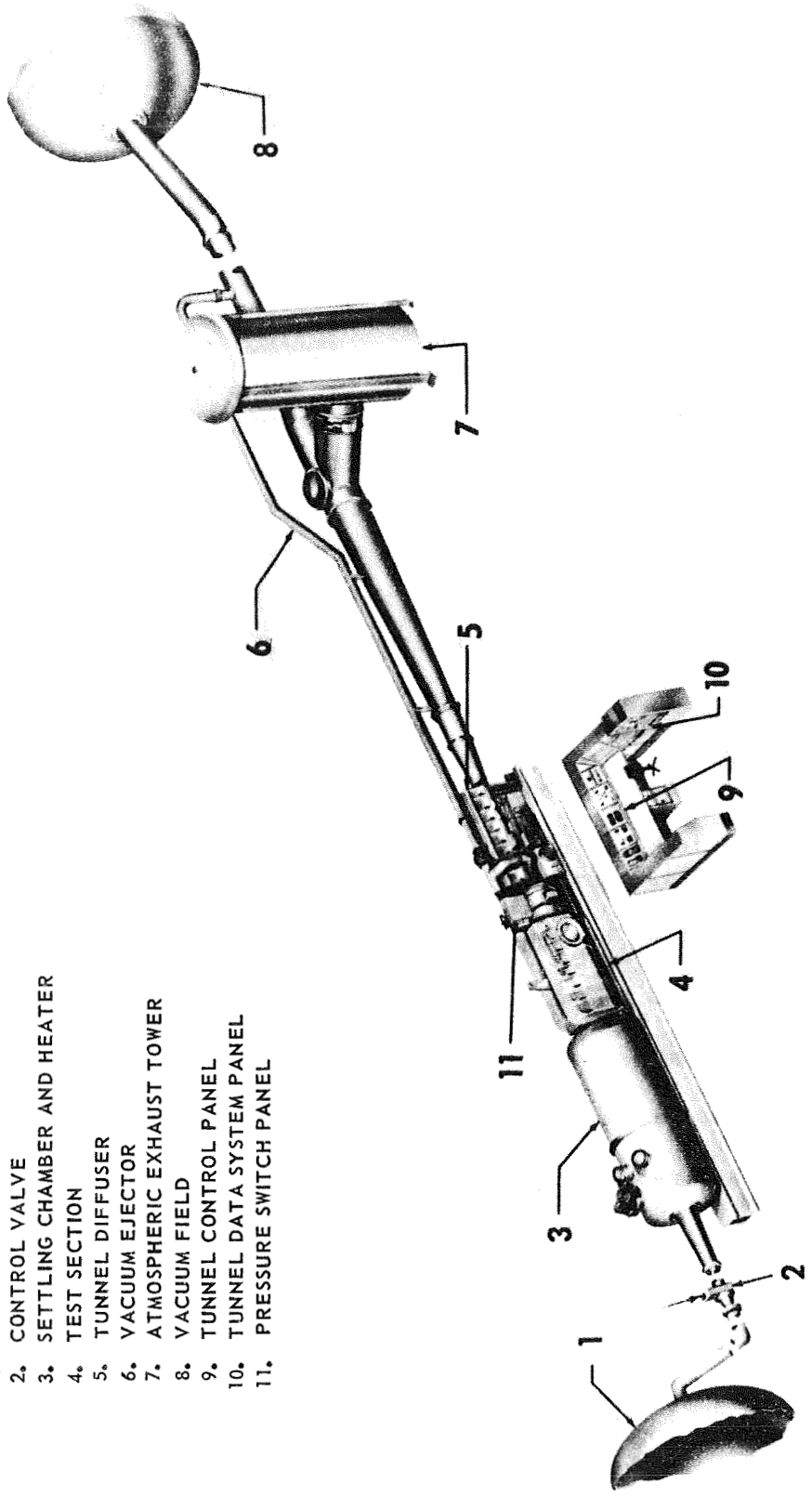

Figure A-1. 14- BY 14-INCH TRISONIC WIND TUNNEL LAYOUT

Tunnel flow is exhausted through an acoustically damped tower into the atmosphere or into the vacuum field of 42,000 cubic feet. The vacuum tanks are evacuated by vacuum pumps driven by a total of 500 hp.

Data are recorded by a solid state digital data acquisition system. The digitized data are transferred to punch cards during the run to be reduced later by a computer to proper coefficient form. A description of the data system and data reduction procedures is presented in references 5 and 6, respectively.

The tunnel components and performance are discussed in more detail in references 7 and 8.

A.2 PICTORIAL REVIEW OF MODELS AND TEST SECTION

Figures A-2 and A-3 depict the boundary layer and 90-degree-step model installed in the test section. Also, a detailed view of the plastic outerwall extension can be observed.

Figure A-4 shows console arrangement with the special test section in the background. A view of the rake probe for total pressure measurements are presented in Figure A-5. Figure A-6 shows the hollow model extension attached to the downstream end of the special test section plug. A view of the boundary layer model without the outerwall extension is shown in Figure A-7.

Figures A-8 and A-9 show details of transducer amplifiers, the soft-mounted bar and static orifices.

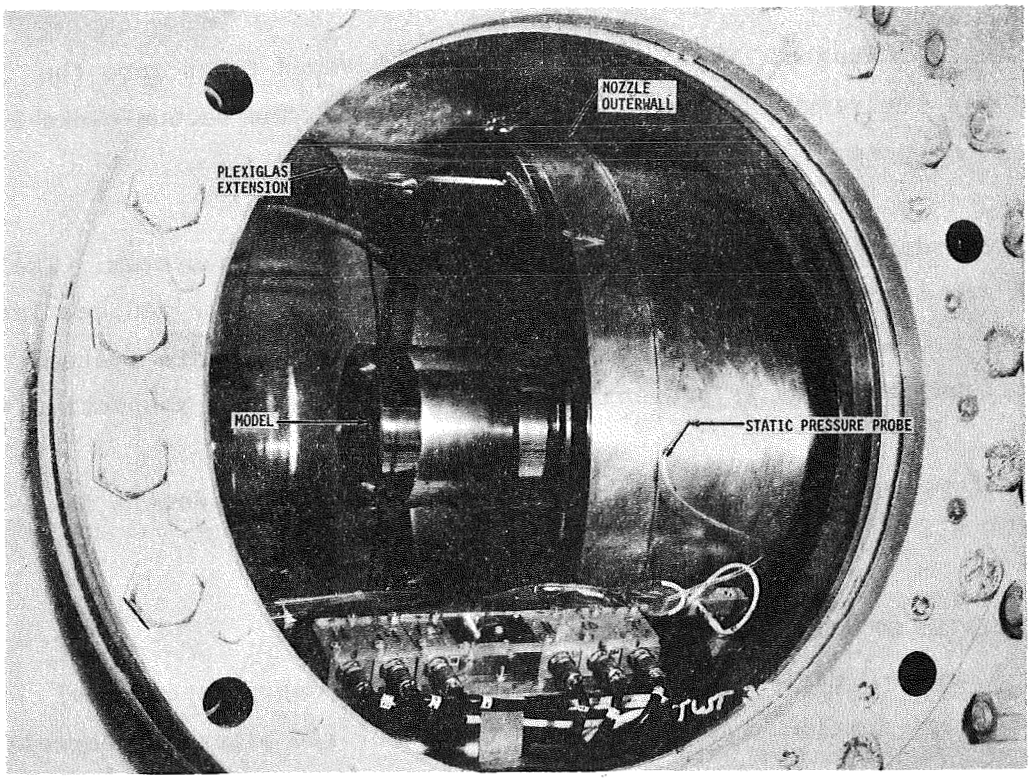

Figure A-2. BOUNDARY LAYER MODEL WITH PLASTIC OUTERWALL EXTENSION, INSTALLED

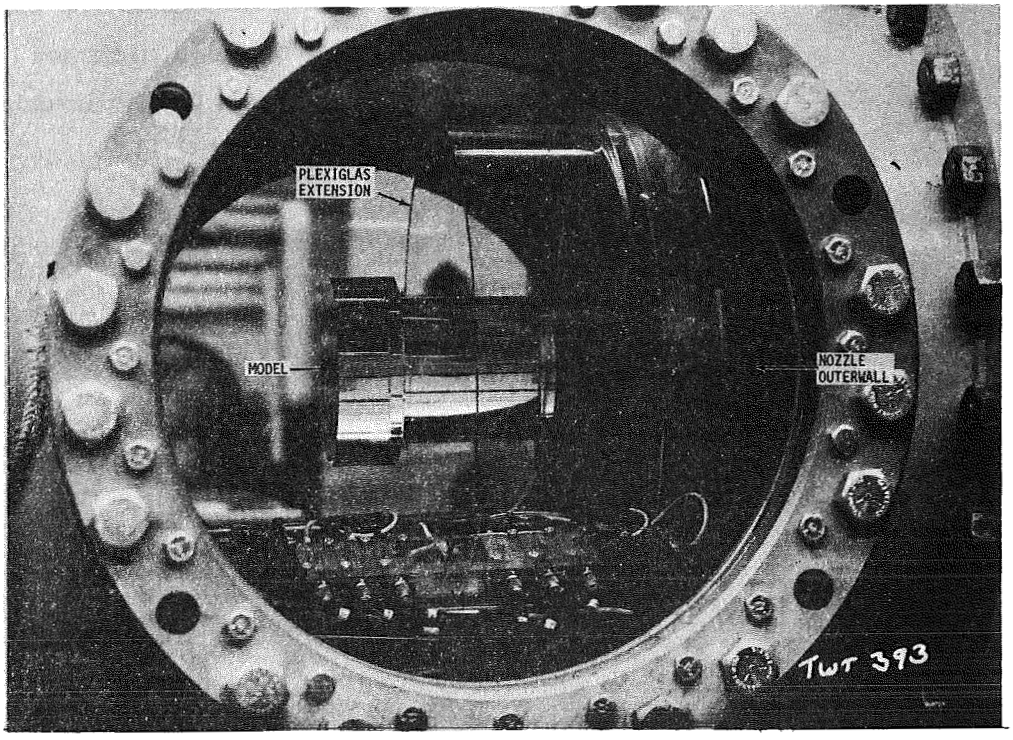

Figure A-3. 90° STEP MODEL WITH PLASTIC OUTERWALL EXTENSION, INSTALLED

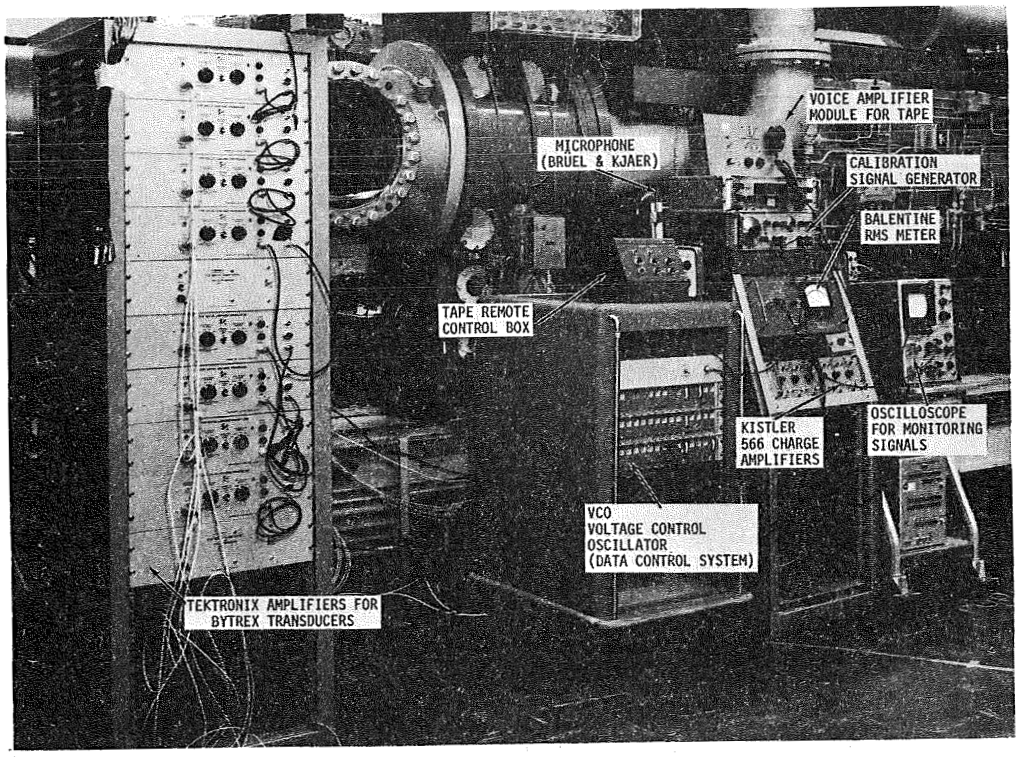

Figure A-4. DATA ACQUISITION AND MONITORING CONSOLE ARRANGEMENT

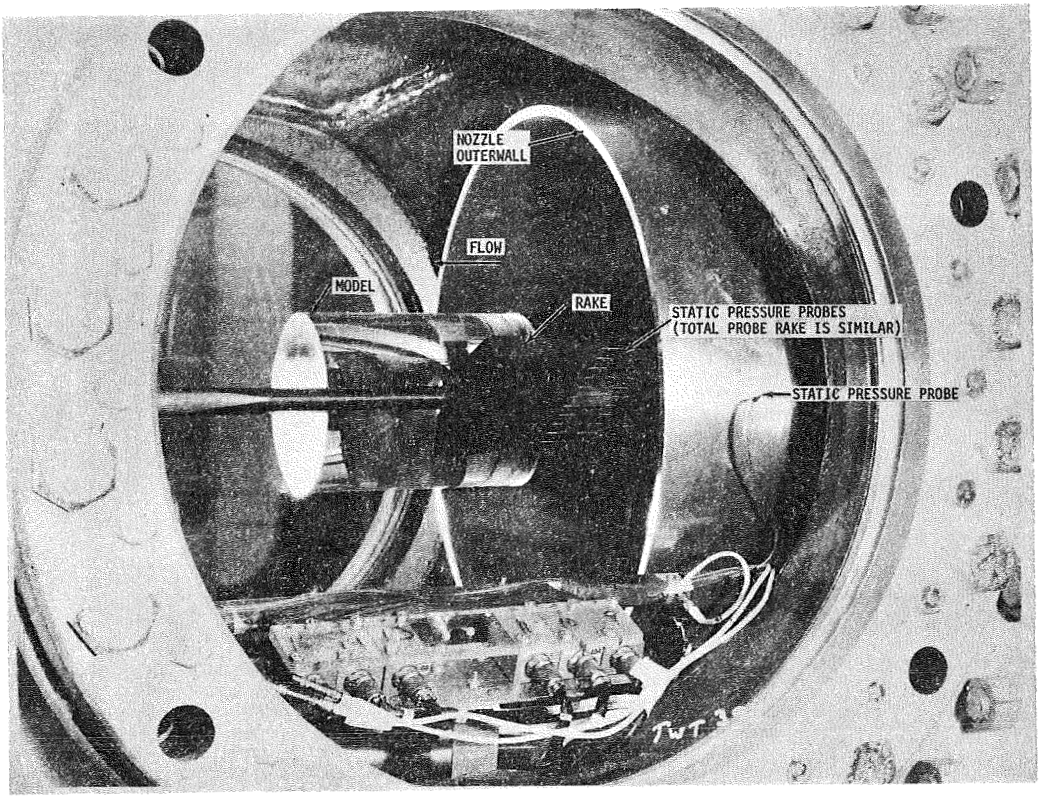

Figure A-5. PROBE RAKE INSIDE TEST SECTION

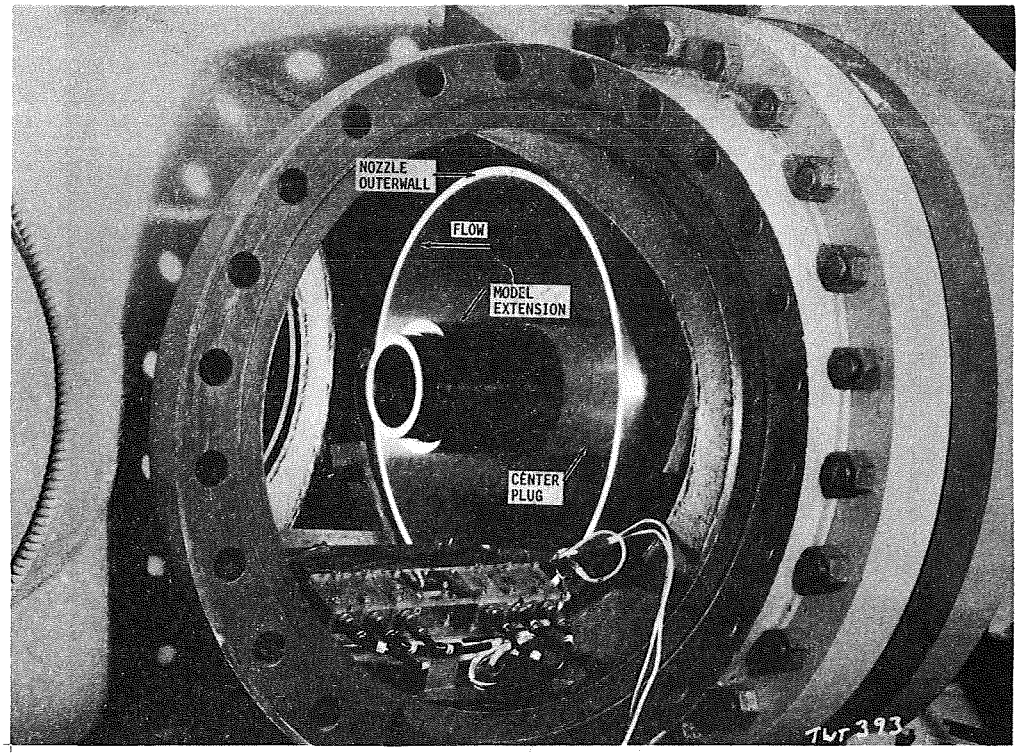

Figure A-6. DETAIL OF THREADED MODEL EXTENSION AND CENTER PLUG MOUNT

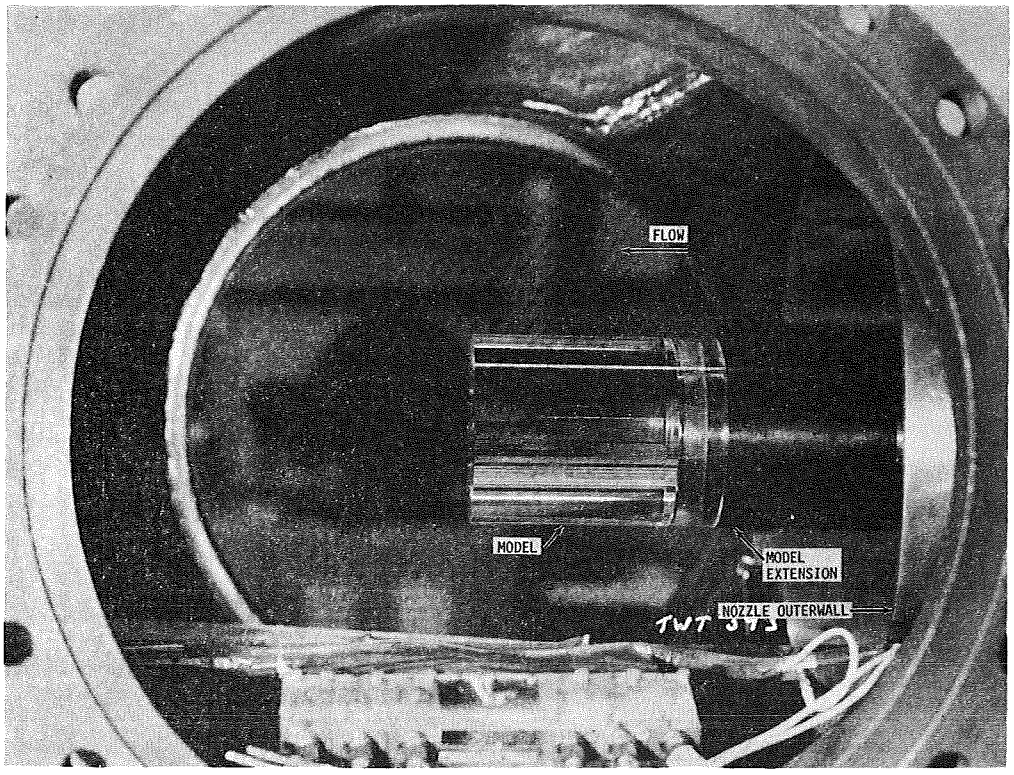

Figure A-7. BOUNDARY LAYER MODEL INSIDE TEST SECTION

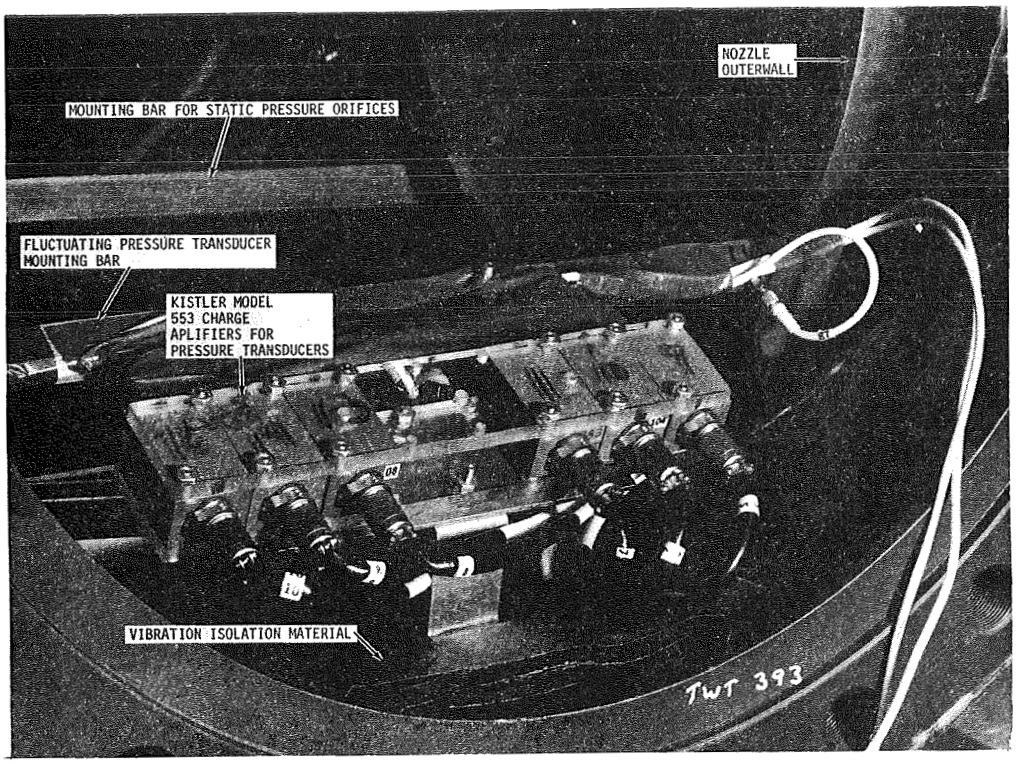

Figure A-8. DETAIL OF TRANSDUCER CHARGE AMPLIFIERS MOUNTED INSIDE TEST SECTION

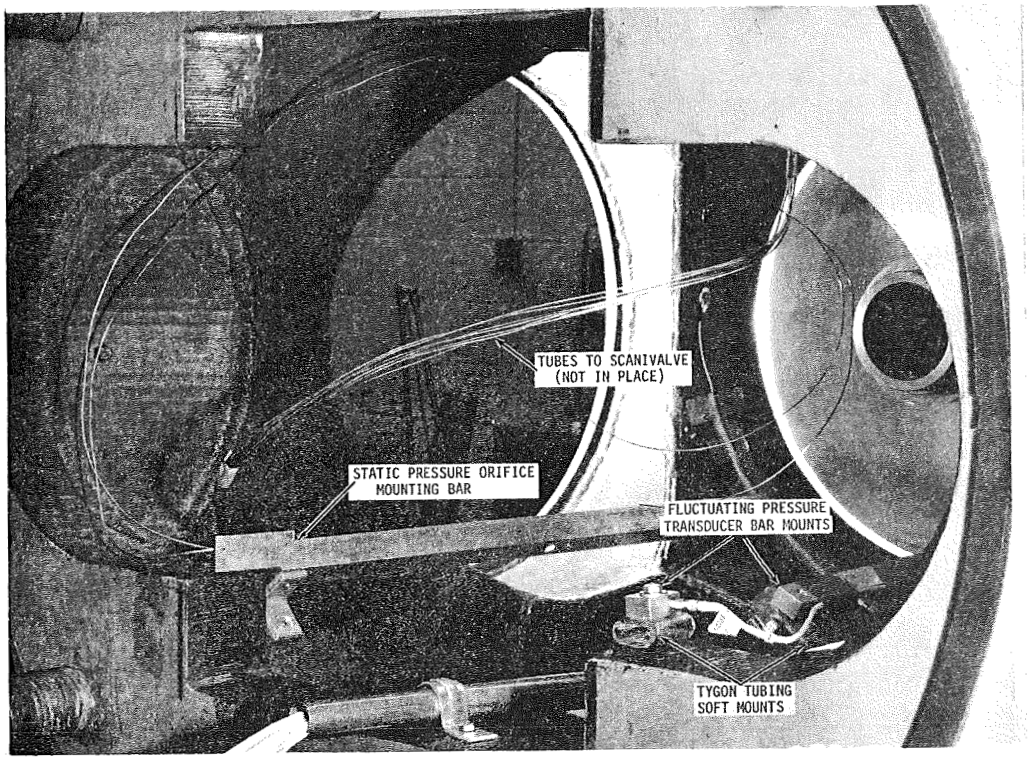

Figure A-9. DETAIL OF STATIC AND FLUCTUATING PRESSURE INSTRUMENTATION BAR MOUNTS INSIDE TEST SECTION

MSFC - SSA, Ala